

REVIEW ARTICLE

Some Recent Advances on Spectral Methods for Unbounded Domains

Jie Shen^{1,*} and Li-Lian Wang²

¹ *Department of Mathematics, Purdue University, West Lafayette, IN, 47907, USA.*

² *Division of Mathematical Sciences, School of Physical and Mathematical Sciences, Nanyang Technological University, 637616, Singapore.*

Received 13 January 2008; Accepted (in revised version) 8 June 2008

Available online 1 August 2008

Abstract. We present in this paper a unified framework for analyzing the spectral methods in unbounded domains using mapped Jacobi, Laguerre and Hermite functions. A detailed comparison of the convergence rates of these spectral methods for solutions with typical decay behaviors is carried out, both theoretically and computationally. A brief review on some of the recent advances in the spectral methods for unbounded domains is also presented.

AMS subject classifications: 65N35, 65N22, 65F05, 35J05

Key words: Spectral method, unbounded domain, orthogonal polynomials, rational functions, Hermite functions, Laguerre functions.

Contents

1	Introduction	196
2	Mapped Jacobi methods	197
3	Laguerre spectral methods	210
4	Hermite spectral methods	223
5	Implementations, numerical results and discussions	230
6	Miscellaneous issues and extensions	233
7	Concluding remarks	237

*Corresponding author. *Email addresses:* shen@math.purdue.edu (J. Shen), lilian@ntu.edu.sg (L. Wang)

1 Introduction

Spectral methods for solving PDEs on unbounded domains can be essentially classified into four approaches:

(i) Domain truncation: truncate unbounded domains to bounded domains and solve the PDEs on bounded domains supplemented with artificial or transparent boundary conditions (see, e.g., [17, 21, 22, 25, 44, 51]);

(ii) Approximation by classical orthogonal systems on unbounded domains, e.g., Laguerre or Hermite polynomials/functions (see, e.g., [7, 14, 20, 30, 31, 36, 43, 47]);

(iii) Approximation by other, non-classical orthogonal systems (see, e.g., [14]), or by mapped orthogonal systems, e.g., image of classical Jacobi polynomials through a suitable mapping (see, e.g. [32, 34, 35, 54]);

(iv) Mapping: map unbounded domains to bounded domains and use standard spectral methods to solve the mapped PDEs in the bounded domains (see, e.g., [9–12, 15, 24, 26]).

Boyd provided in [11] an excellent review on general properties and practical implementations for many of these approaches. In general, the domain truncation approach is only a viable option for problems with rapidly (exponentially) decaying solutions or when accurate non-reflecting or exact boundary conditions are available at the truncated boundary. On the other hand, with proper choices of mappings and/or scaling parameters, the other three approaches can all be effectively applied to a variety of problems with rapid or slow decaying (or even growing) solutions. Since there is a vast literature on domain truncations, particularly for Helmholtz equations and Maxwell equations for scattering problems and the analysis involved is very different from the other three approaches, the domain truncation approach will not be addressed in this paper.

We note that the last two approaches are mathematically equivalent (see Section 2.5.1 for more details) but their computational implementations are different. More precisely, the last approach involves solving the mapped PDEs (which are often cumbersome to deal with) using classical Jacobi polynomials while the third approach solves the original PDE using the mapped Jacobi polynomials. The main advantage of the last approach is that it can be implemented and analyzed using standard procedures and approximation results, but its main disadvantage is that the transformed equation is usually very complicated which, in many cases, makes its implementation and analysis unusually cumbersome. On the other hand, we work on the original PDE in the third approach and approximate its solution by using a new family of orthogonal functions which are images of classical Jacobi polynomials under a suitable mapping. The analysis of this approach will require approximation results by the new family of orthogonal functions. The main advantage is that once these approximation results are established, they can be directly applied to a large class of problems. Thus, we shall mainly concentrate on the second and third approaches, and provide a general framework for the analysis of these spectral methods.

While spectral methods have been used for solving PDEs on unbounded domains

for over thirty years, and there have been several isolated efforts in the early years on the error analysis of these methods (see, e.g. [6, 7, 15, 20, 23, 42]), it is only in the last ten years or so that the basic approximation properties of these orthogonal systems, and their applications to PDEs, were systematically studied (cf. [13] for a brief account). However, many of these analyses use different approaches and involve complicated Sobolev spaces, making it hard for non-experts to extract useful information from these error estimates and to carry out error analysis for their applications. The main purposes of this paper are three folds: (i) to present a unified framework, for the analysis of mapped Jacobi, Laguerre and Hermite spectral methods, which leads to more concise results (than those appeared in the literature) and optimal approximation results in most situations; (ii) to make a detailed comparison on the convergence rates of different methods for several typical solutions; and (iii) to provide a brief (by no means complete) review on some of the recent work for the analysis and application of spectral methods in unbounded domains.

This paper is organized as follows. In the next section, we consider the mapped spectral methods and present a unified framework to study their convergence properties. In Section 3, we consider the approximation by the (generalized) Laguerre polynomials/functions, and Section 4 is devoted to the approximation by the Hermite polynomials/functions. These three sections are presented with a unified style and encompass most of the important approximation results on these orthogonal systems developed in the last few years. In Section 5, we provide some implementation details and compare the performances of different methods with two typical examples. In Section 6, we discuss various extensions and other issues related to the applications of these spectral methods. We end this paper with a few concluding remarks.

We now introduce some notations. Let $\omega(x)$ be a certain weight function in $\Omega := (a, b)$, where a or b could be infinite. We shall use the weighted Sobolev spaces $H_{\omega}^r(\Omega)$ ($r = 0, 1, 2, \dots$), whose inner products, norms and semi-norms are denoted by $(\cdot, \cdot)_{r, \omega}$, $\|\cdot\|_{r, \omega}$ and $|\cdot|_{r, \omega}$, respectively. For real $r > 0$, we define the space $H_{\omega}^r(\Omega)$ by space interpolation. In particular, the norm and inner product of $L_{\omega}^2(\Omega) = H_{\omega}^0(\Omega)$ are denoted by $\|\cdot\|_{\omega}$ and $(\cdot, \cdot)_{\omega}$, respectively. The subscript ω will be omitted from the notations in case of $\omega \equiv 1$. For notational convenience, we denote $\partial_x^k = d^k / dx^k$, $k \geq 1$, and for any nonnegative integer N , let P_N be the set of all algebraic polynomials of degree $\leq N$. We denote by c a generic positive constant independent of any function and N , and use the expression $A \lesssim B$ to mean that there exists a generic positive constant c such that $A \leq cB$.

2 Mapped Jacobi methods

A common and effective strategy in dealing with an unbounded domain is to use a suitable mapping that transforms an infinite domain to a finite domain. Then, images of classical orthogonal polynomials under the inverse mapping will form a set of orthogonal basis functions which can be used to approximate solutions of PDEs in the infinite domains.

Early practitioners of this approach include Grosch & Orszag [24] and Boyd [8]. The book by Boyd [11] contains an extensive review on many practical aspects of the mapped spectral methods. In the last couple of years, a series of papers have been devoted to the convergence analysis of the mapped spectral methods (see, e.g., [34, 35, 39, 54]).

We present below a general framework for the analysis and implementations of the mapped spectral methods.

To study the properties of the mapped Jacobi approximations, we recall some basic properties and results for the classical Jacobi polynomials $J_n^{\alpha, \beta}(y)$, $y \in I := (-1, 1)$, $n \geq 0$.

2.1 Some results on Jacobi approximations

Let $\omega^{\alpha, \beta}(y) = (1-y)^\alpha(1+y)^\beta$ be the Jacobi weight function. For $\alpha, \beta > -1$, the Jacobi polynomials are mutually orthogonal in $L^2_{\omega^{\alpha, \beta}}(I)$, i.e.,

$$\int_I J_n^{\alpha, \beta}(y) J_m^{\alpha, \beta}(y) \omega^{\alpha, \beta}(y) dy = \gamma_n^{\alpha, \beta} \delta_{n, m}, \quad (2.1)$$

where $\delta_{n, m}$ is the Kronecker function, and

$$\gamma_n^{\alpha, \beta} = \frac{2^{\alpha+\beta+1} \Gamma(n+\alpha+1) \Gamma(n+\beta+1)}{(2n+\alpha+\beta+1) \Gamma(n+1) \Gamma(n+\alpha+\beta+1)}. \quad (2.2)$$

They are eigenfunctions of the Sturm-Liouville problem:

$$\partial_y((1-y)^{\alpha+1}(1+y)^{\beta+1} \partial_y J_n^{\alpha, \beta}(y)) + \lambda_n^{\alpha, \beta} (1-y)^\alpha (1+y)^\beta J_n^{\alpha, \beta}(y) = 0, \quad (2.3)$$

with the eigenvalues:

$$\lambda_n^{\alpha, \beta} = n(n+\alpha+\beta+1), \quad n \geq 0, \alpha, \beta > -1. \quad (2.4)$$

Now, we define the $L^2_{\omega^{\alpha, \beta}}(I)$ -orthogonal projection: $\hat{\pi}_N^{\alpha, \beta}: L^2_{\omega^{\alpha, \beta}}(I) \rightarrow P_N$, such that

$$(\hat{\pi}_N^{\alpha, \beta} v - v, v_N)_{\omega^{\alpha, \beta}} = 0, \quad \forall v_N \in P_N. \quad (2.5)$$

Define the weighted space

$$\hat{B}_{\alpha, \beta}^m(I) := \{v \in L^2_{\omega^{\alpha, \beta}}(I) : \partial_y^k v \in L^2_{\omega^{\alpha+k, \beta+k}}(I), 0 \leq k \leq m\}. \quad (2.6)$$

The following result was proved in [19] (see also [3, 38]):

Lemma 2.1.

$$\|\partial_y^l(\hat{\pi}_N^{\alpha, \beta} v - v)\|_{\omega^{\alpha+l, \beta+l}} \lesssim N^{l-m} \|\partial_y^m v\|_{\omega^{\alpha+m, \beta+m}}, \quad 0 \leq l \leq m, \forall v \in \hat{B}_{\alpha, \beta}^m(I). \quad (2.7)$$

Let $\mathcal{I}_N^{\alpha, \beta}$ be the Jacobi-Gauss or Jacobi-Gauss-Radau interpolation operator. The following interpolation approximation result can be found in [38].

Lemma 2.2. For any $v \in \hat{B}_{\alpha, \beta}^m(I)$ with $m \geq 1$,

$$\begin{aligned} & \|\partial_y(\mathcal{I}_N^{\alpha, \beta} v - v)\|_{\omega^{\alpha+1, \beta+1}} + N \|\mathcal{I}_N^{\alpha, \beta} v - v\|_{\omega^{\alpha, \beta}} \\ & \lesssim N^{1-m} \|\partial_y^m v\|_{\omega^{\alpha+m, \beta+m}}. \end{aligned} \quad (2.8)$$

2.2 Mappings

Let us consider a family of mappings of the form:

$$x = g(y; s), \quad s > 0, y \in I := (-1, 1), x \in \Lambda := (0, +\infty) \text{ or } (-\infty, +\infty), \quad (2.9)$$

such that

$$\begin{aligned} \frac{dx}{dy} &= g'(y; s) > 0, \quad s > 0, y \in I, \\ g(-1; s) &= 0, g(1; s) = +\infty, \quad \text{if } \Lambda = (0, +\infty), \\ g(\pm 1; s) &= \pm\infty, \quad \text{if } \Lambda = (-\infty, +\infty). \end{aligned} \quad (2.10)$$

In this one-to-one transform, the parameter s is a positive scaling factor. Without loss of generality, we further assume that the mapping is explicitly invertible, and denote its inverse mapping by

$$y = g^{-1}(x; s) := h(x; s), \quad x \in \Lambda, y \in I, s > 0. \quad (2.11)$$

Several typical mappings that have been proposed and used in practice are of the above type (see, e.g., [11] and the references therein):

- Mappings between $x \in \Lambda = (-\infty, +\infty)$ and $y \in I = (-1, 1)$ with $s > 0$:

- Algebraic mapping:

$$x = \frac{sy}{\sqrt{1-y^2}}, \quad y = \frac{x}{\sqrt{x^2+s^2}}. \quad (2.12)$$

- Logarithmic mapping:

$$x = \text{sarctanh}(y) = \frac{s}{2} \ln \frac{1+y}{1-y}, \quad y = \tanh(s^{-1}x). \quad (2.13)$$

- Exponential mapping:

$$x = \sinh(sy), \quad y = \frac{1}{s} \ln(x + \sqrt{x^2+1}), \quad y \in (-1, 1), x \in (-L_s, L_s), \quad (2.14)$$

where $L_s = \sinh(s)$.

- Mappings between $x \in \Lambda = (0, +\infty)$ and $y \in I = (-1, 1)$ with $s > 0$:

- Algebraic mapping:

$$x = \frac{s(1+y)}{1-y}, \quad y = \frac{x-s}{x+s}. \quad (2.15)$$

– Logarithmic mapping:

$$x = s \operatorname{arctanh}\left(\frac{y+1}{2}\right) = \frac{s}{2} \ln \frac{3+y}{1-y}, \quad y = 1 - 2 \tanh(s^{-1}x). \quad (2.16)$$

– Exponential mapping:

$$x = \sinh\left(\frac{s}{2}(1+y)\right), \quad y = \frac{2}{s} \ln(x + \sqrt{x^2+1}) - 1, \quad (2.17)$$

where $y \in (-1, 1)$ and $x \in (0, L_s)$ with $L_s = \sinh(s)$.

The special feature which distinguishes these mappings is that, as $|y| \rightarrow \pm 1$, x varies algebraically, logarithmically or exponentially for algebraic, logarithmic or exponential mappings, respectively. The parameter s is a scaling/stretching factor which can be used to fine tune the spacing of collocation points. We also notice that the image of the exponential mappings (2.14) and (2.17) is a finite interval, so they combine both mapping and domain truncation.

2.3 Mapped Jacobi approximations

Given a mapping $x = g(y; s)$ satisfying (2.9)–(2.11) and a family of orthogonal polynomials $\{p_k(y)\}$ with $y \in I = (-1, 1)$, $\{p_k(h(x; s))\}$ forms a new family of orthogonal functions in $\Lambda = (0, \infty)$ or $(-\infty, \infty)$. For example, the algebraic mappings (2.12) or (2.15) with the Chebyshev or Legendre polynomials lead to orthogonal rational basis functions which have been studied in [8, 9, 14, 34, 35, 40].

For the sake of generality, we consider the mapped Jacobi approximations. Let $J_k^{\alpha, \beta}(y)$ ($\alpha, \beta > -1$) be the k -th degree classical Jacobi polynomials whose properties are summarized in the Appendix. We define the mapped Jacobi polynomials as

$$j_{s,n}^{\alpha, \beta}(x) := J_n^{\alpha, \beta}(y) = J_n^{\alpha, \beta}(h(x; s)), \quad x \in \Lambda, y \in I. \quad (2.18)$$

We infer from (2.1) that (2.18) defines a new family of orthogonal functions $\{j_{s,n}^{\alpha, \beta}\}$ in $L^2_{\omega_s^{\alpha, \beta}}(\Lambda)$, i.e.,

$$\int_{\Lambda} j_{s,n}^{\alpha, \beta}(x) j_{s,m}^{\alpha, \beta}(x) \omega_s^{\alpha, \beta}(x) dx = \gamma_n^{\alpha, \beta} \delta_{m,n}, \quad (2.19)$$

where the constant $\gamma_n^{\alpha, \beta}$ is given in (2.2), and the weight function

$$\omega_s^{\alpha, \beta}(x) = \omega^{\alpha, \beta}(y) \frac{dy}{dx} = \omega^{\alpha, \beta}(y) (g'(y; s))^{-1} > 0, \quad (2.20)$$

with $y = h(x; s)$ and $\omega^{\alpha, \beta}(y) = (1-y)^\alpha (1+y)^\beta$.

We now present some approximation properties of these mapped Jacobi polynomials. Let us define the finite dimensional approximation space

$$V_{s,N}^{\alpha, \beta} = \operatorname{span}\{j_{s,n}^{\alpha, \beta}(x) : n = 0, 1, \dots, N\}, \quad (2.21)$$

and consider the orthogonal projection $\pi_{N,s}^{\alpha,\beta} : L^2_{\omega_s^{\alpha,\beta}}(\Lambda) \rightarrow V_{s,N}^{\alpha,\beta}$ such that

$$(\pi_{N,s}^{\alpha,\beta} u - u, v_N)_{\omega_s^{\alpha,\beta}} = 0, \quad \forall v_N \in V_{s,N}^{\alpha,\beta}. \tag{2.22}$$

Thanks to the orthogonality, we can write

$$(\pi_{N,s}^{\alpha,\beta} u)(x) = \sum_{n=0}^N \hat{u}_{s,n}^{\alpha,\beta} j_{s,n}^{\alpha,\beta}(x), \tag{2.23}$$

where

$$\hat{u}_{s,n}^{\alpha,\beta} = \frac{1}{\gamma_n^{\alpha,\beta}} \int_{\Lambda} u(x) j_{s,n}^{\alpha,\beta}(x) \omega_s^{\alpha,\beta}(x) dx.$$

We now introduce a weighted space which is particularly suitable to describe the L^2 -projection errors. Given a mapping satisfying (2.9)–(2.11), we set

$$a_s(x) := \frac{dx}{dy} (> 0), \quad U_s(y) := u(x) = u(g(y;s)). \tag{2.24}$$

The key to express the error estimates in a concise form is to introduce an operator

$$D_x u := a_s \frac{du}{dx}.$$

One verifies readily that

$$\frac{dU_s}{dy} = a_s \frac{du}{dx} = D_x u, \quad \frac{d^2 U_s}{dy^2} = a_s \frac{d}{dx} \left(a_s \frac{du}{dx} \right) = D_x^2 u,$$

and an induction argument leads to

$$\frac{d^k U_s}{dy^k} = a_s \underbrace{\frac{d}{dx} \left(a_s \frac{d}{dx} \left(\dots \left(a_s \frac{du}{dx} \right) \dots \right) \right)}_{k-1 \text{ parentheses}} := D_x^k u. \tag{2.25}$$

Let us define

$$\tilde{B}_{\alpha,\beta}^m(\Lambda) = \{ u : u \text{ is measurable in } \Lambda \text{ and } \|u\|_{\tilde{B}_{\alpha,\beta}^m} < \infty \}$$

equipped with the norm and semi-norm

$$\|u\|_{\tilde{B}_{\alpha,\beta}^m} = \left(\sum_{k=0}^m \|D_x^k u\|_{\omega_s^{\alpha+k,\beta+k}}^2 \right)^{\frac{1}{2}}, \quad |u|_{\tilde{B}_{\alpha,\beta}^m} = \|D_x^m u\|_{\omega_s^{\alpha+m,\beta+m}},$$

where the weight function $\omega_s^{\alpha+k,\beta+k}$ is defined in (2.20). We have the following fundamental results for the mapped Jacobi approximations.

Theorem 2.1. *If $u \in \widetilde{B}_{\alpha,\beta}^m(\Lambda)$, we have that for $m \geq 0$,*

$$\|\pi_{s,N}^{\alpha,\beta}u - u\|_{\omega_s^{\alpha,\beta}} \lesssim N^{-m} \|D_x^m u\|_{\omega_s^{\alpha+m,\beta+m}}, \tag{2.26}$$

and for $m \geq 1$,

$$\|\partial_x(\pi_{s,N}^{\alpha,\beta}u - u)\|_{\omega_s^{\alpha,\beta}} \lesssim N^{1-m} \|D_x^m u\|_{\omega_s^{\alpha+m,\beta+m}}, \tag{2.27}$$

where

$$\widetilde{\omega}_s^{\alpha,\beta}(x) = \omega^{\alpha+1,\beta+1}(y)g'(y;s), \quad y = h(x;s).$$

Proof. Let $U_s(y) = u(x) = u(h(y;s))$ whose Jacobi expansion is $U_s(y) = \sum_{n=0}^{\infty} \widehat{U}_{s,n}^{\alpha,\beta} J_n^{\alpha,\beta}(y)$. Then, by the definition (2.18), we have the relation between the coefficients of the Jacobi and mapped Jacobi expansions:

$$\widehat{u}_{s,n}^{\alpha,\beta} = \frac{1}{\gamma_n^{\alpha,\beta}} (u, j_{s,n}^{\alpha,\beta})_{\omega_s^{\alpha,\beta}} = \frac{1}{\gamma_n^{\alpha,\beta}} (U_s, J_n^{\alpha,\beta})_{\omega^{\alpha,\beta}} = \widehat{U}_{s,n}^{\alpha,\beta}. \tag{2.28}$$

Let $\widehat{\pi}_N^{\alpha,\beta}$ be the $L_{\omega^{\alpha,\beta}}^2$ -orthogonal projection operator associated with the Jacobi polynomials (cf. (2.5)). By (2.1), (2.19) and Lemma 2.1,

$$\begin{aligned} \|\pi_{s,N}^{\alpha,\beta}u - u\|_{\omega_s^{\alpha,\beta}}^2 &= \sum_{n=N+1}^{\infty} (\widehat{u}_{s,n}^{\alpha,\beta})^2 \gamma_n^{\alpha,\beta} = \sum_{n=N+1}^{\infty} (\widehat{U}_{s,n}^{\alpha,\beta})^2 \gamma_n^{\alpha,\beta} \\ &= \|\widehat{\pi}_N^{\alpha,\beta}U_s - U_s\|_{\omega^{\alpha,\beta}}^2 \lesssim N^{-2m} \|\partial_y^m U_s\|_{\omega^{\alpha+m,\beta+m}}^2 \\ &\lesssim N^{-2m} \|D_x^m u\|_{\omega_s^{\alpha+m,\beta+m}}^2. \end{aligned} \tag{2.29}$$

Next, we deduce from (2.18) and the orthogonality of $\{\partial_y J_n^{\alpha,\beta}\}$ that $\{\partial_x j_{s,n}^{\alpha,\beta}\}$ is $L_{\widetilde{\omega}_s^{\alpha,\beta}}^2$ -orthogonal, and

$$\|\partial_x j_{s,n}^{\alpha,\beta}\|_{\widetilde{\omega}_s^{\alpha,\beta}}^2 = \|\partial_y J_n^{\alpha,\beta}\|_{\omega^{\alpha+1,\beta+1}}^2 = \lambda_n^{\alpha,\beta} \gamma_n^{\alpha,\beta},$$

where $\lambda_n^{\alpha,\beta}$ is the eigenvalue of the Jacobi Sturm-Liouville problem (cf. (2.4)). Therefore, by (2.28) and Lemma 2.1,

$$\begin{aligned} \|\partial_x(\pi_{s,N}^{\alpha,\beta}u - u)\|_{\widetilde{\omega}_s^{\alpha,\beta}}^2 &= \sum_{n=N+1}^{\infty} \lambda_n^{\alpha,\beta} \gamma_n^{\alpha,\beta} (\widehat{u}_{s,n}^{\alpha,\beta})^2 = \sum_{n=N+1}^{\infty} \lambda_n^{\alpha,\beta} \gamma_n^{\alpha,\beta} (\widehat{U}_{s,n}^{\alpha,\beta})^2 \\ &= \|\partial_y(\pi_N^{\alpha,\beta}U_s - U_s)\|_{\omega^{\alpha+1,\beta+1}}^2 \lesssim N^{2(1-m)} \|\partial_y^m U_s\|_{\omega^{\alpha+m,\beta+m}}^2 \\ &\lesssim N^{2(1-m)} \|D_x^m u\|_{\omega_s^{\alpha+m,\beta+m}}^2. \end{aligned} \tag{2.30}$$

This ends the proof. □

Remark 2.1. It should be pointed out that under the above general settings, the approximation results on the higher-order projections, such as the $H_{\omega_s}^{1,\alpha,\beta}(\Lambda)$ – orthogonal projection $\pi_{s,N}^{1,\alpha,\beta} : H_{\omega_s}^{1,\alpha,\beta}(\Lambda) \rightarrow V_{s,N}^{\alpha,\beta}$, can be established by using the existing Jacobi approximation results (see, e.g., [38]) and a similar argument as above.

In particular, applying the above results with $\alpha=\beta=0, -1/2$ to the algebraic mappings (2.12) and (2.15) leads to more concise and in some cases improved, Chebyshev and Legendre rational approximation results which were developed separately in [34, 35, 39, 54].

The error estimates in the above theorem look very similar to the usual spectral error estimates in a finite interval (cf. Lemma 2.1). First of all, it is clear from the above theorem that the projection error converges faster than any algebraic rate if a function decays exponentially fast at infinity. For a function with singularities inside the domain, the above theorem and Lemma 2.1 lead to the same order of convergence, assuming that the function decays sufficiently fast at infinity. However, for a given smooth function, they may lead to very different convergence rates due to the difference in the norms used to measure the regularity.

We now determine the convergence rates for three sets of functions with typical decay properties:

Set 1. Exponential decay with oscillation at infinity

$$u(x) = \sin kx e^{-x} \text{ for } x \in (0, \infty) \text{ or } u(x) = \sin kx e^{-x^2} \text{ for } x \in (-\infty, \infty). \quad (2.31)$$

Set 2. Algebraic decay without oscillation at infinity

$$u(x) = (1+x)^{-h} \text{ for } x \in (0, \infty) \text{ or } u(x) = (1+x^2)^{-h} \text{ for } x \in (-\infty, \infty). \quad (2.32)$$

Set 3. Algebraic decay with oscillation at infinity

$$u(x) = \frac{\sin kx}{(1+x)^h} \text{ for } x \in (0, \infty) \text{ or } u(x) = \frac{\sin kx}{(1+x^2)^h} \text{ for } x \in (-\infty, \infty). \quad (2.33)$$

Consider first the mapping (2.15). Then,

$$D_x = \left(\frac{dy}{dx}\right)^{-1} \frac{d}{dx} = \frac{(x+s)^2}{2s} \frac{d}{dx}, \quad \omega_s^{k,l}(x) = \left(\frac{2s}{x+s}\right)^k \left(\frac{2x}{x+s}\right)^l \frac{2s}{(x+s)^2}.$$

Hence, for $u(x) = (1+x)^{-h}$, it can be easily checked that $\|D_x^m u\|_{\omega_s^{\alpha+m,\beta+m}} < \infty$ if $m < 2h + \alpha + 1$, which implies that

$$\|u - \pi_N^{\alpha,\beta} u\|_{\omega_s^{\alpha,\beta}} \lesssim N^{-(2h+\alpha+1)} \quad (u(x) = (1+x)^{-h}). \quad (2.34)$$

On the other hand, for $u(x) = \sin kx \cdot (1+x)^{-h}$, it can also be easily checked that $\|D_x^m u\|_{\omega_s^{\alpha+m, \beta+m}} < \infty$ if $m < \frac{2h+\alpha+1}{3}$, which implies that

$$\|u - \pi_N^{\alpha, \beta} u\|_{\omega_s^{\alpha, \beta}} \lesssim N^{-(2h+\alpha+1)/3} \quad \left(u(x) = \frac{\sin kx}{(1+x)^h}\right). \tag{2.35}$$

Next, we consider the mapping (2.12) which leads to

$$D_x = \left(\frac{dy}{dx}\right)^{-1} \frac{d}{dx} = \frac{(x^2+s^2)^{3/2}}{s^2} \frac{d}{dx'}$$

$$\omega_s^{k,l}(x) = \left(\frac{\sqrt{x^2+s^2}-x}{\sqrt{x^2+s^2}}\right)^k \left(\frac{\sqrt{x^2+s^2}+x}{\sqrt{x^2+s^2}}\right)^l \frac{s^2}{(x^2+s^2)^{3/2}}.$$

Hence, for $u(x) = (1+x^2)^{-h}$, we have $\|D_x^m u\|_{\omega_s^{\alpha+m, \beta+m}} < \infty$ if $m < 2h+\alpha+1$, which implies that

$$\|u - \pi_N^{\alpha, \beta} u\|_{\omega_s^{\alpha, \beta}} \lesssim N^{-(2h+\alpha+1)} \quad (u(x) = (1+x^2)^{-h}). \tag{2.36}$$

On the other hand, for $u(x) = \sin kx \cdot (1+x^2)^{-h}$, we have $\|D_x^m u\|_{\omega_s^{\alpha+m, \beta+m}} < \infty$ if $m < \frac{2h+\alpha+1}{2}$, which implies that

$$\|u - \pi_N^{\alpha, \beta} u\|_{\omega_s^{\alpha, \beta}} \lesssim N^{-(2h+\alpha+1)/2} \quad \left(u(x) = \frac{\sin kx}{(1+x^2)^h}\right). \tag{2.37}$$

A few remarks are in order: (i) If h is a positive integer, then $u(x) = (1+x)^{-h}$ and $u(x) = (1+x^2)^{-h}$ are rational functions and they can be expressed **exactly** by a finite sum of mapped rational functions; (ii) For other cases, only algebraic convergence rates are achievable even though the functions are smooth; (iii) the convergence rate for solutions with oscillation at infinities is much slower than that for solutions without oscillation at infinities; and (iv) For solutions with exponential decay at infinity, the convergence rate will be faster than any algebraic rate; numerical results in [34, 35, 54] (see also [11]) indicate that the convergence rate is sub-geometrical as $e^{-c\sqrt{N}}$; and (v) numerical results performed in [34, 35, 39, 54] are consistent with the estimates in (2.34)-(2.37).

2.4 Mapped Jacobi interpolation approximations

We now consider the Gauss and Gauss-Radau quadrature formulas on unbounded domains based on the mapped Jacobi polynomials. To fix the idea, we only consider the Gauss quadrature, since the Gauss-Radau quadrature (which is useful in the semi-infinite interval) can be treated in exactly the same fashion. Let $\{\xi_{N,j}^{\alpha, \beta}, \omega_{N,j}^{\alpha, \beta}\}_{j=0}^N$ be the Jacobi-Gauss nodes and weights, and there holds

$$\int_{-1}^1 \phi(y) \omega^{\alpha, \beta}(y) dy = \sum_{j=0}^N \phi(\xi_{N,j}^{\alpha, \beta}) \omega_{N,j}^{\alpha, \beta}, \quad \forall \phi \in P_{2N+1}. \tag{2.38}$$

Applying a mapping (2.9) to the above leads to the mapped Jacobi-Gauss quadrature:

$$\int_{\Lambda} u(x)\omega_s^{\alpha,\beta}(x)dx = \sum_{j=0}^N u(\zeta_{s,N,j}^{\alpha,\beta})\rho_{s,N,j}^{\alpha,\beta} \quad \forall u \in V_{s,2N+1}^{\alpha,\beta}, \tag{2.39}$$

where

$$\zeta_{s,N,j}^{\alpha,\beta} := g(\zeta_{N,j}^{\alpha,\beta};s), \quad \rho_{s,N,j}^{\alpha,\beta} := \omega_{N,j}^{\alpha,\beta}, \quad 0 \leq j \leq N \tag{2.40}$$

are the mapped Jacobi-Gauss nodes and weights.

Accordingly, we can define the discrete inner product and discrete norm:

$$(u,v)_{\omega_s^{\alpha,\beta},N} = \sum_{j=0}^N u(\zeta_{s,N,j}^{\alpha,\beta})v(\zeta_{s,N,j}^{\alpha,\beta})\rho_{s,N,j}^{\alpha,\beta} \quad \|u\|_{\omega_s^{\alpha,\beta},N} = (u,u)_{\omega_s^{\alpha,\beta},N}^{\frac{1}{2}} \quad \forall u,v \in C(\Lambda).$$

The mapped Jacobi-Gauss interpolation operator $\mathcal{I}_{s,N}^{\alpha,\beta} : C(\Lambda) \rightarrow V_{s,N}^{\alpha,\beta}$ is defined by

$$\mathcal{I}_{s,N}^{\alpha,\beta} u \in V_{s,N}^{\alpha,\beta} \quad \text{such that} \quad (\mathcal{I}_{s,N}^{\alpha,\beta} u)(\zeta_{s,N,j}^{\alpha,\beta}) = u(\zeta_{s,N,j}^{\alpha,\beta}), j=0,1,\dots,N. \tag{2.41}$$

Let $\mathcal{I}_N^{\alpha,\beta}$ be the Jacobi-Gauss (or Jacobi-Gauss-Radau) interpolation operator. By definition, we have

$$\mathcal{I}_{s,N}^{\alpha,\beta} u(x) = (\mathcal{I}_N^{\alpha,\beta} U_s)(y) = (\mathcal{I}_N^{\alpha,\beta} U_s)(h(x;s)). \tag{2.42}$$

Then, we can easily derive the following results by combining Lemma 2.2 and Theorem 2.1.

Theorem 2.2. *If $u \in \widetilde{B}_{\alpha,\beta}^m(\Lambda)$ with $m \geq 1$, then*

$$\|\partial_x(\mathcal{I}_{s,N}^{\alpha,\beta} u - u)\|_{\omega_s^{\alpha,\beta}} + N\|\mathcal{I}_{s,N}^{\alpha,\beta} u - u\|_{\omega_s^{\alpha,\beta}} \lesssim N^{1-m}\|D_x^m u\|_{\omega_s^{\alpha+m,\beta+m}}. \tag{2.43}$$

We now examine how the mapping parameter s affects the distribution of the nodes. Assume that the nodes $\{\zeta_{s,N,j}^{\alpha,\beta}\}_{j=0}^N$ are arranged in ascending order. We first observe that by the mean value theorem,

$$\zeta_{s,N,j+1}^{\alpha,\beta} - \zeta_{s,N,j}^{\alpha,\beta} = g'(\zeta;s)(\zeta_{s,N,j+1}^{\alpha,\beta} - \zeta_{s,N,j}^{\alpha,\beta}), \tag{2.44}$$

for certain $\zeta \in (\zeta_{s,N,j}^{\alpha,\beta}, \zeta_{s,N,j+1}^{\alpha,\beta})$. Hence, the intensity of stretching essentially depends on the derivative values of the mapping. For the mappings (2.13), (2.12), (2.16) and (2.15), we have

$$\frac{dx}{dy} = g'(y;s) = \frac{s}{1-y^2}, \quad \frac{s}{(1-y^2)^{3/2}}, \quad \frac{2s}{(3+y)(1-y)}, \quad \frac{2s}{(1-y)^2}, \tag{2.45}$$

respectively. Therefore, the grid is stretched more and more as s increases.

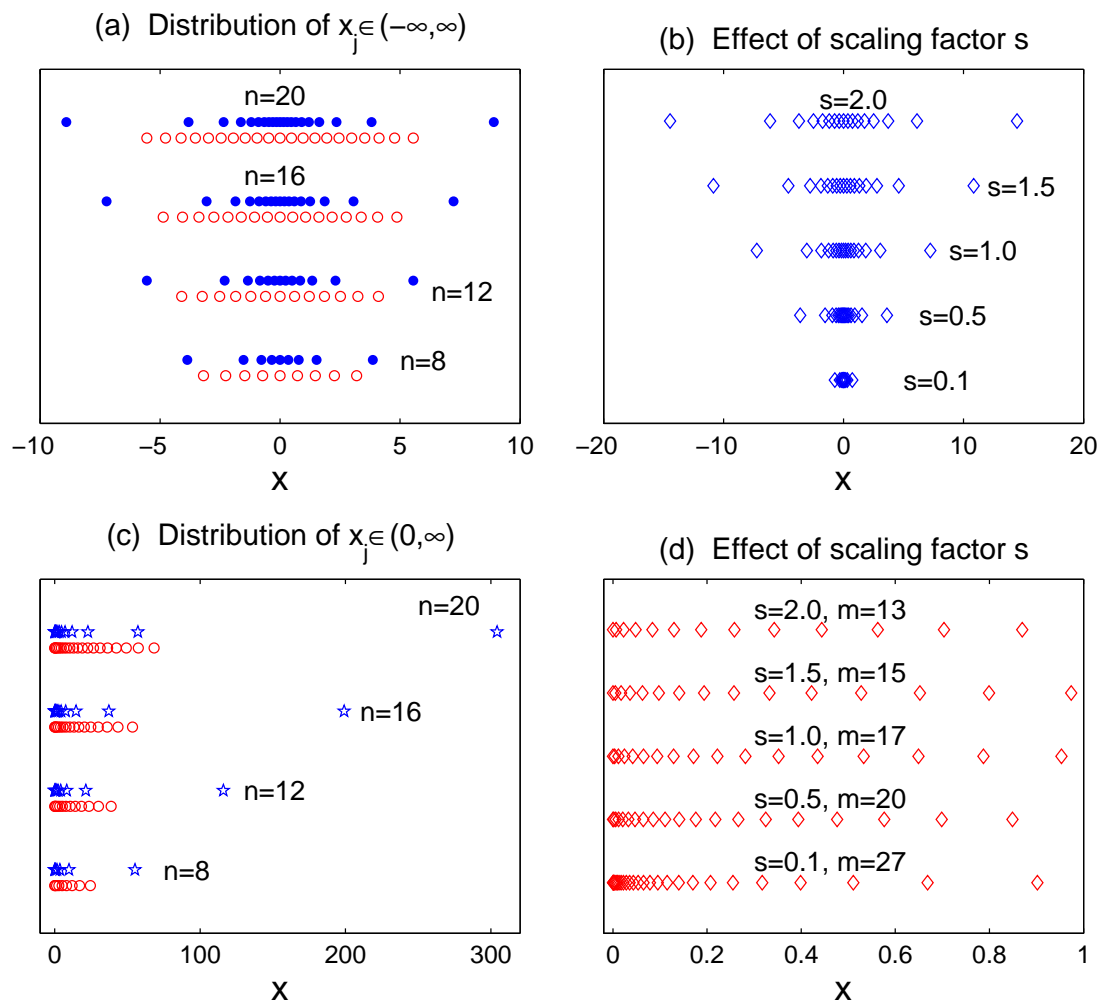


Figure 1: (a) Hermite-Gauss points ("o") vs. mapped Legendre-Gauss points using the algebraic map (2.12) with $s=1$ ("•") for various n ; (b) Mapped Legendre-Gauss points with $n=16$ and various scaling factor s ; (c) Laguerre-Gauss-Radau points ("o") vs. mapped Legendre-Gauss-Radau points using the algebraic map (2.15) with $s=1$ ("*") for various n ; (d) Mapped Legendre-Gauss-Radau points with $n=32$ and various scaling factor s (m is the number of points in the subinterval $[0,1)$).

In Fig. 1, we plot sample grid distributions for different scaling factors with various numbers of nodes for the mapped Legendre Gauss (or Gauss-Radau) points (see the caption for details).

A comparison with Hermite-Gauss points is also presented in Fig. 1(a). We notice that the mapped Legendre-Gauss points are more clustered near the origin and spread further, while the Hermite-Gauss points are more evenly distributed. It should be observed that the distribution of mapped Legendre-Gauss points is more favorable since a much larger effective interval is covered. However, it can be shown that in both cases,

the smallest distance between neighboring points is $\mathcal{O}(N^{-1})$, as opposed to $\mathcal{O}(N^{-2})$ for Jacobi-Gauss type nodes in a finite interval.

A comparison of mapped Legendre and Laguerre Gauss-Radau nodes is shown in Fig. 1(c). The mapped Legendre-Gauss-Radau points are much more clustered near the origin, and one can check that the smallest distance between neighboring points is $\mathcal{O}(N^{-2})$, as opposed to $\mathcal{O}(N^{-1})$ for the Laguerre Gauss-Radau nodes. Hence, the distribution of mapped Legendre-Gauss-Radau points is more favorable as far as resolution/accuracy is concerned but it will lead to a more restrictive CFL condition if explicit schemes are used for time-dependent problems.

2.5 Numerical methods using mapped Jacobi polynomials

2.5.1 A generic example

Consider the model equation

$$\gamma u - \partial_x(a(x)\partial_x u) = f, \quad x \in \Lambda = (-\infty, +\infty), \quad \gamma \geq 0, \quad (2.46)$$

with suitable decay conditions at $\pm\infty$ which will depend on the weight function in the weighted variational formulation.

For a given mapping $x=g(y;s)$ with $x \in \Lambda$ and $y \in (-1,1)$, we recall that the mapped Jacobi polynomials are mutually orthogonal in $L^2_{\omega_s^{\alpha,\beta}}(\Lambda)$. Hence, the mapped Jacobi method for (2.46) is to find $u_N \in V_{s,N}^{\alpha,\beta}$ such that

$$\gamma(u_N, v_N)_{\omega_s^{\alpha,\beta}} + (a(x)\partial_x u_N, \partial_x(v_N \omega_s^{\alpha,\beta})) = (\mathcal{I}_{s,N}^{\alpha,\beta} f, v_N)_{\omega_s^{\alpha,\beta}}, \quad \forall v_N \in V_{s,N}^{\alpha,\beta}. \quad (2.47)$$

Let us now consider the second approach described in the introduction. Here, Eq. (2.46) is first transformed into

$$\gamma U_s - \frac{1}{g'(y;s)} \partial_y \left(\frac{a(g(y;s))}{g'(y;s)} \partial_y U_s \right) = F_s, \quad (2.48)$$

where $U_s(y) = u(g(y;s))$ and $F_s(y) = f(g(y;s))$.

Then, let $\hat{\omega}_s^{\alpha,\beta}(y) = \omega^{\alpha,\beta}(y)g'(y;s)$, the Jacobi spectral method for (2.48) is to find $\tilde{u}_N \in P_N$ such that

$$\gamma(\tilde{u}_N, \tilde{v}_N)_{\omega^{\alpha,\beta}} + \left(\frac{a(g(y;s))}{g'(y;s)} \partial_y \tilde{u}_N, \partial_y(\tilde{v}_N \hat{\omega}_s^{\alpha,\beta}) \right) = (\mathcal{I}_N^{\alpha,\beta} F_s, \tilde{v}_N)_{\omega^{\alpha,\beta}}, \quad \forall \tilde{v}_N \in P_N. \quad (2.49)$$

One can verify easily that $\tilde{u}_N(y) = u_N(g(y;s))$. Hence, the two approaches are mathematically equivalent.

We remark that the formulation (2.49) is in general more difficult to analyze due to the singular nature of $g'(y;s)$, while the analysis for the formulation (2.47) becomes standard once we establish the basic approximation properties of the mapped Jacobi polynomials.

On the other hand, Eq. (2.48) can be easily implemented using the standard Jacobi-collocation (or more specifically Chebyshev-collocation) method. Indeed, let $\{h_{j,N}(y)\}_{1 \leq j \leq N}$ be the Lagrange polynomials associated with the Jacobi-Gauss points $\{y_j\}_{1 \leq j \leq N}$, the Jacobi-collocation approximation to (2.48) is to find $U_{s,N}(y) = \sum_{j=1}^N u_j h_{j,N}(y)$ such that

$$\gamma U_{s,N}(y_j) - \left(\frac{1}{g'(y_j;s)} \partial_y \left(\frac{a(g(y;s))}{g'(y;s)} \partial_y U_{s,N} \right) \right) (y_j) = F_s(y_j), \quad 1 \leq j \leq N. \tag{2.50}$$

Let us denote

$$\begin{aligned} \mathbf{u} &= (u_1, \dots, u_N)^t, \quad \mathbf{f} = (F_s(y_1), \dots, F_s(y_N))^t, \quad D_{ij} = h'_j(y_i), \quad D = (D_{ij}), \\ \Lambda_i &= \frac{a(g(y_i;s))}{g'(y_i;s)}, \quad \Lambda = \text{diag}(\Lambda_i), \quad \Sigma_i = \frac{1}{g'(y_i;s)}, \quad \Sigma = \text{diag}(\Sigma_i). \end{aligned}$$

Then, (2.50) leads to the matrix system

$$(\gamma I - \Sigma D \Lambda D) \mathbf{u} = \mathbf{f},$$

which can be easily solved by using a standard linear algebra routine. Note that in the above procedure, we only need to compute the Jacobi-Gauss points $\{y_j\}_{1 \leq j \leq N}$ and the associated differentiation matrix D whose entries can be found for instance in [19].

2.5.2 Error estimates for a model problem

We consider the Jacobi rational approximation to the model problem

$$\begin{aligned} \gamma u(x) - \partial_x^2 u(x) &= f(x), \quad x \in \Lambda = (0, \infty), \\ u(0) &= 0, \end{aligned} \tag{2.51}$$

with a suitable decay condition at infinity which is to be determined by the weak formulation of (2.51).

For a given mapping, let $\omega = \omega_s^{\alpha, \beta}$ be the weight function associated with the mapped Jacobi polynomials, and denote

$$H_{0,\omega}^1(\Lambda) = \{u \in H_\omega^1(\Lambda) : u(0) = 0\}.$$

We define a bilinear form

$$a_\omega(v, \phi) = \gamma(v, \phi)_\omega + (\partial_x v, \partial_x(\phi \omega)), \quad \forall u, v \in H_{0,\omega}^1(\Lambda).$$

Then, a weak formulation for (2.51) is to find $u \in H_{0,\omega}^1(\Lambda)$ such that

$$a_\omega(u, v) = (f, v)_\omega, \quad \forall v \in H_{0,\omega}^1(\Lambda), \tag{2.52}$$

for $f \in (H_{0,\omega}^1(\Lambda))'$. Note that $u \in H_{0,\omega}^1(\Lambda)$ implies a decay condition for u at infinity.

Let us denote $X_N = \{u \in V_{s,N}^{\alpha,\beta} : u(0) = 0\}$. We can then define the Galerkin approximation of (2.52) by the mapped Jacobi polynomials as follows: For $f \in L^2_\omega(\Lambda) \cap C(\bar{\Lambda})$, find $u_N \in X_N$ such that

$$a_\omega(u_N, v_N) = (\mathcal{I}_{s,N}^{\alpha,\beta} f, v_N)_\omega, \quad \forall v_N \in X_N. \tag{2.53}$$

Unlike the standard spectral method in a finite domain, the well-posedness of (2.52) and of (2.53) is not guaranteed for all cases with $\gamma \geq 0$. A general result for the well-posedness of an abstract equation of the form (2.52) is established in [49]. For the readers' convenience, we recall this result below (cf. Lemma 2.3 in [49]):

Lemma 2.3. *We assume that*

$$d_1 = \max_{x \in \bar{\Lambda}} |\omega^{-1}(x) \partial_x \omega(x)|, \quad d_2 = \max_{x \in \bar{\Lambda}} |\omega^{-1}(x) \partial_x^2 \omega(x)|$$

are finite and that $u^2(x) \omega'(x)|_{x \in \partial\Lambda} = 0$ for $u \in H^1_{0,\omega}(\Lambda)$. Then, for any $u, v \in H^1_\omega(\Lambda)$, we have that

$$a_\omega(u, v) \leq (d_1 + 1) \|u\|_{1,\omega} \|v\|_{1,\omega} + \gamma \|u\|_\omega \|v\|_\omega, \tag{2.54}$$

and for any $v \in H^1_{0,\omega}(\Lambda)$,

$$a_\omega^{(v)}(v, v) \geq \|v\|_{1,\omega}^2 + (\gamma - d_2/2) \|v\|_\omega^2. \tag{2.55}$$

Remark 2.2. The inequality (2.55) is derived under a general framework. For a specific problem, the constant $\gamma - d_2/2$ can often be replaced by a larger constant.

Thanks to the above lemma, it is then straightforward to prove the following general result:

Theorem 2.3. *Assume that the conditions of Lemma (2.3) are satisfied and $\gamma - d_2/2 > 0$. Then the problem (2.52) (resp. (2.53)) admits a unique solution. Furthermore, we have the error estimate:*

$$\|u - u_N\|_{1,\omega} \lesssim \inf_{v_N \in X_N} \|u - v_N\|_{1,\omega} + \|f - \mathcal{I}_{s,N}^{\alpha,\beta} f\|_\omega. \tag{2.56}$$

Remark 2.3. With a change of variable x to x/c ($c > 0$) for Eq. (2.46), the restriction on γ can be relaxed to $\gamma > 0$.

Hence, given a mapping and a pair of Jacobi parameters (α, β) , we just need to compute upper bounds for d_1 and d_2 , verify that the conditions of Theorem 2.3 are satisfied, and apply the approximation results in Theorems 2.1 and 2.2 to (2.56) to get the desired error estimates.

Consider for example the mapped Legendre method for (2.52) with the mapping (2.15). It can be shown that for this mapping, we have $d_1 \leq 2$ and $d_2 \leq 6$. Applying Theorems 2.1 and 2.2 to (2.56) with $(\alpha, \beta) = (0, 0)$ leads to the following results:

Corollary 2.1. Let u and u_N be the solutions of (2.52) and (2.53) with $(\alpha, \beta) = (0, 0)$ and the mapping (2.15) with $s = 1$. Assume that $u \in \tilde{B}_{0,0}^m(\Lambda)$, $f \in \tilde{B}_{0,0}^k(\Lambda)$ and $\gamma > 3$. We have

$$\|u - u_N\|_{1, \omega_1^{0,0}} \lesssim N^{1-m} \|D_x^m u\|_{\omega_1^{m,m}} + N^{-k} \|D_x^k f\|_{\omega_1^{k,k}}. \quad (2.57)$$

We note that a slightly improved condition on γ was derived in [35] using a refined estimate for (2.55).

A similar procedure can be applied to the mapped Chebyshev method for (2.52) with the mapping (2.15). Note however that in this case we have $d_1, d_2 = \infty$. Nevertheless, one can still show that $a_\omega(\cdot, \cdot)$ is continuous and coercive (cf. [34]). Applying Theorems 2.1 and 2.2 to (2.56) with $(\alpha, \beta) = (-\frac{1}{2}, -\frac{1}{2})$ leads to the following results (cf. [34]):

Corollary 2.2. Let u and u_N be the solutions of (2.52) and (2.53) with $(\alpha, \beta) = (-\frac{1}{2}, -\frac{1}{2})$ and the mapping (2.15) with $s = 1$. Assuming that $u \in \tilde{B}_{-1/2, -1/2}^m(\Lambda)$ and $f \in \tilde{B}_{-1/2, -1/2}^k(\Lambda)$ and that $\gamma > \frac{14}{27}$. We have

$$\|u - u_N\|_{1, \omega_1^{-1/2, -1/2}} \lesssim N^{1-m} \|D_x^m u\|_{\omega_1^{m-1/2, m-1/2}} + N^{-k} \|D_x^k f\|_{\omega_1^{k-1/2, k-1/2}}. \quad (2.58)$$

Remark 2.4. Error estimates which are essentially equivalent to (2.57) and (2.58) but in different forms were derived in [34, 35].

The same procedure can be used to derive error estimates on mapped Jacobi methods for problems in the whole line (cf. [39, 54]).

3 Laguerre spectral methods

For problems in a semi-infinite interval, it is natural to use (generalized) Laguerre polynomials/functions which form orthonormal basis in (weighted) Sobolev spaces.

3.1 Generalized Laguerre approximations

We first recall some basic properties of generalized Laguerre polynomials/functions.

3.1.1 Generalized Laguerre polynomials

Let $\Lambda := (0, \infty)$. The generalized Laguerre polynomials (GLPs), denoted by $\mathcal{L}_n^{(\alpha)}(x)$ ($\alpha > -1$), are the eigenfunctions of the Sturm-Liouville problem

$$x^{-\alpha} e^x \partial_x (x^{\alpha+1} e^{-x} \partial_x \mathcal{L}_n^{(\alpha)}(x)) + \lambda_n \mathcal{L}_n^{(\alpha)}(x) = 0, \quad x \in \Lambda, \quad (3.1)$$

with the eigenvalues $\lambda_n = n$. Compared with the Jacobi polynomials in a finite interval, the linear growth of λ_n for the Laguerre polynomial indicates, on the one hand, a slower convergence rate of the Laguerre expansion, but on the other hand, leads to better inverse inequalities and consequently milder CFL conditions for time dependent problems.

The GLPs are mutually orthogonal in $L^2_{\omega_\alpha}(\Lambda)$ with the weight function $\omega_\alpha(x) = x^\alpha e^{-x}$, i.e.,

$$\int_0^{+\infty} \mathcal{L}_n^{(\alpha)}(x)\mathcal{L}_m^{(\alpha)}(x)\omega_\alpha(x)dx = \gamma_n^{(\alpha)}\delta_{mn} \quad \text{with } \gamma_n^{(\alpha)} = \frac{\Gamma(n+\alpha+1)}{\Gamma(n+1)}. \quad (3.2)$$

The three-term recurrence formula of the GLPs reads

$$\begin{aligned} (n+1)\mathcal{L}_{n+1}^{(\alpha)}(x) &= (2n+\alpha+1-x)\mathcal{L}_n^{(\alpha)}(x) - (n+\alpha)\mathcal{L}_{n-1}^{(\alpha)}(x), \\ \mathcal{L}_0^{(\alpha)}(x) &= 1, \quad \mathcal{L}_1^{(\alpha)}(x) = \alpha+1-x. \end{aligned} \quad (3.3)$$

We infer from (3.1) and (3.2) that

$$\int_0^{+\infty} \partial_x \mathcal{L}_n^{(\alpha)}(x)\partial_x \mathcal{L}_m^{(\alpha)}(x)x\omega_\alpha(x)dx = \lambda_n \gamma_n^{(\alpha)}\delta_{mn}. \quad (3.4)$$

An important property of the GLPs is the following derivative relation:

$$\partial_x \mathcal{L}_n^{(\alpha)}(x) = -\mathcal{L}_{n-1}^{(\alpha+1)}(x) = -\sum_{k=0}^{n-1} \mathcal{L}_k^{(\alpha)}(x). \quad (3.5)$$

The case $\alpha=0$ leads to the classical Laguerre polynomials, which are used most frequently in practice and will simply be denoted by $\mathcal{L}_n(x)$. As in the finite interval case, it is actually easier to study the whole family of generalized Laguerre polynomials, rather than the Laguerre polynomials alone.

3.1.2 Approximation results by generalized Laguerre polynomials

We begin by analyzing the approximation properties of the $L^2_{\omega_\alpha}$ -orthogonal projection $\pi_{N,\alpha}: L^2_{\omega_\alpha}(\Lambda) \rightarrow P_N$, defined by

$$(u - \pi_{N,\alpha}u, v_N)_{\omega_\alpha} = 0, \quad \forall v_N \in P_N. \quad (3.6)$$

It is clear that the polynomial $\pi_{N,\alpha}u$ is the best approximation u in $L^2_{\omega_\alpha}(\Lambda)$, and

$$\pi_{N,\alpha}u(x) = \sum_{n=0}^N \hat{u}_n^{(\alpha)} \mathcal{L}_n^{(\alpha)}(x),$$

with

$$\hat{u}_n^{(\alpha)} = \frac{1}{\gamma_n^{(\alpha)}} \int_0^{+\infty} u(x)\mathcal{L}_n^{(\alpha)}(x)\omega_\alpha(x)dx, \quad n \geq 0.$$

Similar to the Jacobi approximations, we define

$$B_\alpha^m(\Lambda) := \{u : \partial_x^k u \in L^2_{\omega_{\alpha+k}}(\Lambda), 0 \leq k \leq m\}, \quad (3.7)$$

equipped with the norm and semi-norm

$$\|u\|_{B_\alpha^m} = \left(\sum_{k=0}^m \|\partial_x^k u\|_{\omega_{\alpha+k}}^2 \right)^{1/2}, \quad |u|_{B_\alpha^m} = \|\partial_x^m u\|_{\omega_{\alpha+m}}.$$

In particular, we omit the subscript α , when $\alpha = 0$. In contrast to the usual weighted Sobolev space $H_{\omega_\alpha}^m(\Lambda)$, the weight function corresponding to derivative of different order is different in $B_\alpha^m(\Lambda)$.

We observe from (3.5) that

$$\partial_x^k \mathcal{L}_n^{(\alpha)}(x) = (-1)^k \mathcal{L}_{n-k}^{(\alpha+k)}(x), \quad n \geq k, \tag{3.8}$$

and so $\{\partial_x^k \mathcal{L}_n^{(\alpha)}\}$ are orthogonal with respect to the weight $\omega_{\alpha+k}$, i.e.,

$$\int_0^{+\infty} \partial_x^k \mathcal{L}_l^{(\alpha)}(x) \partial_x^k \mathcal{L}_n^{(\alpha)}(x) \omega_{\alpha+k}(x) dx = \gamma_{n-k}^{(\alpha+k)} \delta_{ln}. \tag{3.9}$$

By (3.2) and the Stirling formula,

$$\Gamma(x+1) \sim \sqrt{2\pi} x^{x+1/2} e^{-x}, \quad x \gg 1, \tag{3.10}$$

we have

$$\gamma_{n-k}^{(\alpha+k)} = \frac{\Gamma(n+\alpha+1)}{\Gamma(n-k+1)} \sim n^{\alpha+k}, \quad \text{for } n \gg 1.$$

Summing (3.9) over $0 \leq k \leq m$ leads to

$$\sum_{k=0}^m (\partial_x^k \mathcal{L}_l^{(\alpha)}, \partial_x^k \mathcal{L}_n^{(\alpha)})_{\omega_{\alpha+k}} = 0, \quad \text{if } l \neq n \text{ and } k > \min\{l, n\}$$

which implies that $\{\mathcal{L}_n^{(\alpha)}\}$ are orthogonal in the space $B_\alpha^m(\Lambda)$.

The fundamental generalized Laguerre approximation result is stated below (see, e.g., [19]).

Theorem 3.1. For any $u \in B_\alpha^m(\Lambda)$ and $m \geq 0$,

$$\|\partial_x^l (\pi_{N,\alpha} u - u)\|_{\omega_{\alpha+l}} \lesssim N^{(l-m)/2} \|\partial_x^m u\|_{\omega_{\alpha+m}}, \quad 0 \leq l \leq m. \tag{3.11}$$

Proof. Obviously, we have that

$$\partial_x^l (\pi_{N,\alpha} u - u) = - \sum_{n=N+1}^{\infty} \hat{u}_n^{(\alpha)} \partial_x^l \mathcal{L}_n^{(\alpha)}(x).$$

Hence, by the orthogonality and the Stirling formula (3.10),

$$\begin{aligned} \|\partial_x^l(\pi_{N,\alpha}u - u)\|_{\omega_{\alpha+l}}^2 &= \sum_{n=N+1}^{\infty} \gamma_{n-l}^{(\alpha+l)} |\hat{u}_n^{(\alpha)}|^2 \\ &\leq \max_{n>N} \left\{ \gamma_{n-l}^{(\alpha+l)} / \gamma_{n-m}^{(\alpha+m)} \right\} \sum_{n=N+1}^{\infty} \gamma_{n-m}^{(\alpha+m)} |\hat{u}_n^{(\alpha)}|^2 \\ &\lesssim N^{l-m} \|\partial_x^m u\|_{\omega_{\alpha+m}}^2. \end{aligned}$$

This completes the proof. □

Next, we consider the approximation results for the H^1 -type orthogonal projections. For simplicity, we consider only the usual Laguerre case, i.e., $\alpha = 0$. Hereafter, let $\omega(x) = e^{-x}$ be the usual Laguerre weight function, and denote

$$H_{0,\omega}^1(\Lambda) = \{u \in H_{\omega}^1(\Lambda) : u(0) = 0\}, \quad P_N^0 = \{\phi \in P_N : \phi(0) = 0\}. \tag{3.12}$$

Consider the orthogonal projection $\pi_N^{1,0} : H_{0,\omega}^1(\Lambda) \rightarrow P_N^0$, defined by

$$((u - \pi_N^{1,0}u)', v'_N)_{\omega} = 0, \quad \forall v_N \in P_N^0. \tag{3.13}$$

Theorem 3.2. *If $u \in H_{0,\omega}^1(\Lambda)$ and $\partial_x u \in B_0^{m-1}(\Lambda)$, then for $m \geq 1$,*

$$\|\pi_N^{1,0}u - u\|_{1,\omega} \lesssim N^{\frac{1}{2}-\frac{m}{2}} \|\partial_x^m u\|_{\omega_{m-1}}. \tag{3.14}$$

Proof. Let

$$\phi(x) = \int_0^x \pi_{N-1,0}u'(y)dy.$$

Then $u - \phi \in H_{0,\omega}^1(\Lambda)$. Thanks to the imbedding inequality (see, e.g., [31])

$$\|u\|_{\omega} \lesssim \|\partial_x u\|_{\omega},$$

and Theorem 3.1 with $\alpha = 0$, we find that

$$\|\pi_N^{1,0}u - u\|_{1,\omega} \leq \|\phi - u\|_{1,\omega} \lesssim \|\partial_x(\phi - u)\|_{\omega} \lesssim N^{\frac{1}{2}-\frac{m}{2}} \|\partial_x^m u\|_{\omega_{m-1}}.$$

This ends the proof. □

We note that in general Laguerre polynomials are not good candidates for approximations in infinite domains due to their wild behaviors at infinity. This fact is also reflected in the error estimates in Theorems 3.1 and 3.2. Although these error estimates are also of spectral type, but due to the exponential decay weight in the norm, they only imply meaningful pointwise approximation for a short interval. Hence, the GLPs are only suitable for the approximation of functions with fast algebraic (or exponential) growth at infinity. For problems with some decay properties at infinity, it is more appropriate to use the so called generalized Laguerre functions (GLFs) which we shall consider below.

3.1.3 Generalized Laguerre functions

The generalized Laguerre functions (GLFs) are defined by

$$\widehat{\mathcal{L}}_n^{(\alpha)}(x) := e^{-x/2} \mathcal{L}_n^{(\alpha)}(x), \alpha > -1, x \in \Lambda. \tag{3.15}$$

It is clear that by (3.2), the GLFs are orthogonal with respect to the weight function $\widehat{\omega}_\alpha = x^\alpha$, i.e.,

$$\int_0^{+\infty} \widehat{\mathcal{L}}_n^{(\alpha)}(x) \widehat{\mathcal{L}}_m^{(\alpha)}(x) \widehat{\omega}_\alpha(x) dx = \gamma_n^{(\alpha)} \delta_{mn}, \tag{3.16}$$

where the constant $\gamma_n^{(\alpha)}$ is given in (3.2). In particular, the usual Laguerre functions

$$\widehat{\mathcal{L}}_n(x) = e^{-x/2} \mathcal{L}_n(x), \quad n \geq 0, \quad x \in \Lambda, \tag{3.17}$$

are orthonormal with respect to the uniform weight $\widehat{\omega}_0 \equiv 1$.

As in the last section, we introduce an operator

$$\hat{\partial}_x = \partial_x + \frac{1}{2} \text{ which implies that } \partial_x \mathcal{L}_n^{(\alpha)}(x) = e^{x/2} \hat{\partial}_x \widehat{\mathcal{L}}_n^{(\alpha)}(x). \tag{3.18}$$

It is straightforward to check that the GLFs satisfy the following properties:

- Three-term recurrence relation

$$\begin{aligned} (n+1) \widehat{\mathcal{L}}_{n+1}^{(\alpha)} &= (2n+\alpha+1-x) \widehat{\mathcal{L}}_n^{(\alpha)} - (n+\alpha) \widehat{\mathcal{L}}_{n-1}^{(\alpha)}, \\ \widehat{\mathcal{L}}_0^{(\alpha)} &= e^{-x/2}, \quad \widehat{\mathcal{L}}_1^{(\alpha)} = (\alpha+1-x) e^{-x/2}. \end{aligned} \tag{3.19}$$

- The Sturm-Liouville equation:

$$x^{-\alpha} e^{x/2} \partial_x \left(x^{\alpha+1} e^{-x/2} \hat{\partial}_x \widehat{\mathcal{L}}_n^{(\alpha)}(x) \right) + n \widehat{\mathcal{L}}_n^{(\alpha)}(x) = 0. \tag{3.20}$$

- Orthogonality of the derivative:

$$\int_\Lambda \hat{\partial}_x \widehat{\mathcal{L}}_n^{(\alpha)}(x) \hat{\partial}_x \widehat{\mathcal{L}}_m^{(\alpha)}(x) \widehat{\omega}_{\alpha+1}(x) dx = \lambda_n \gamma_n^{(\alpha)} \delta_{mn}. \tag{3.21}$$

- Some recurrence formulas:

$$\hat{\partial}_x \widehat{\mathcal{L}}_n^{(\alpha)}(x) = -\widehat{\mathcal{L}}_{n-1}^{(\alpha+1)}(x) = -\sum_{k=0}^{n-1} \widehat{\mathcal{L}}_k^{(\alpha)}(x), \tag{3.22a}$$

$$\widehat{\mathcal{L}}_n^{(\alpha)}(x) = \hat{\partial}_x \widehat{\mathcal{L}}_n^{(\alpha)}(x) - \hat{\partial}_x \mathcal{L}_{n+1}^{(\alpha)}(x), \tag{3.22b}$$

$$x \hat{\partial}_x \mathcal{L}_n^{(\alpha)}(x) = n \widehat{\mathcal{L}}_n^{(\alpha)}(x) - (n+\alpha) \widehat{\mathcal{L}}_{n-1}^{(\alpha)}(x). \tag{3.22c}$$

We plot in Fig. 2 some sample graphs of GLPs and GLFs. In contrast to the GLPs, the GLFs are well-behaved with the decay property (see Fig. 2 (d)):

$$|\widehat{\mathcal{L}}_n^{(\alpha)}(x)| \rightarrow 0, \quad \text{as } x \rightarrow +\infty. \tag{3.23}$$

Therefore, the GLPs are suitable for approximation of functions which decay at infinity.

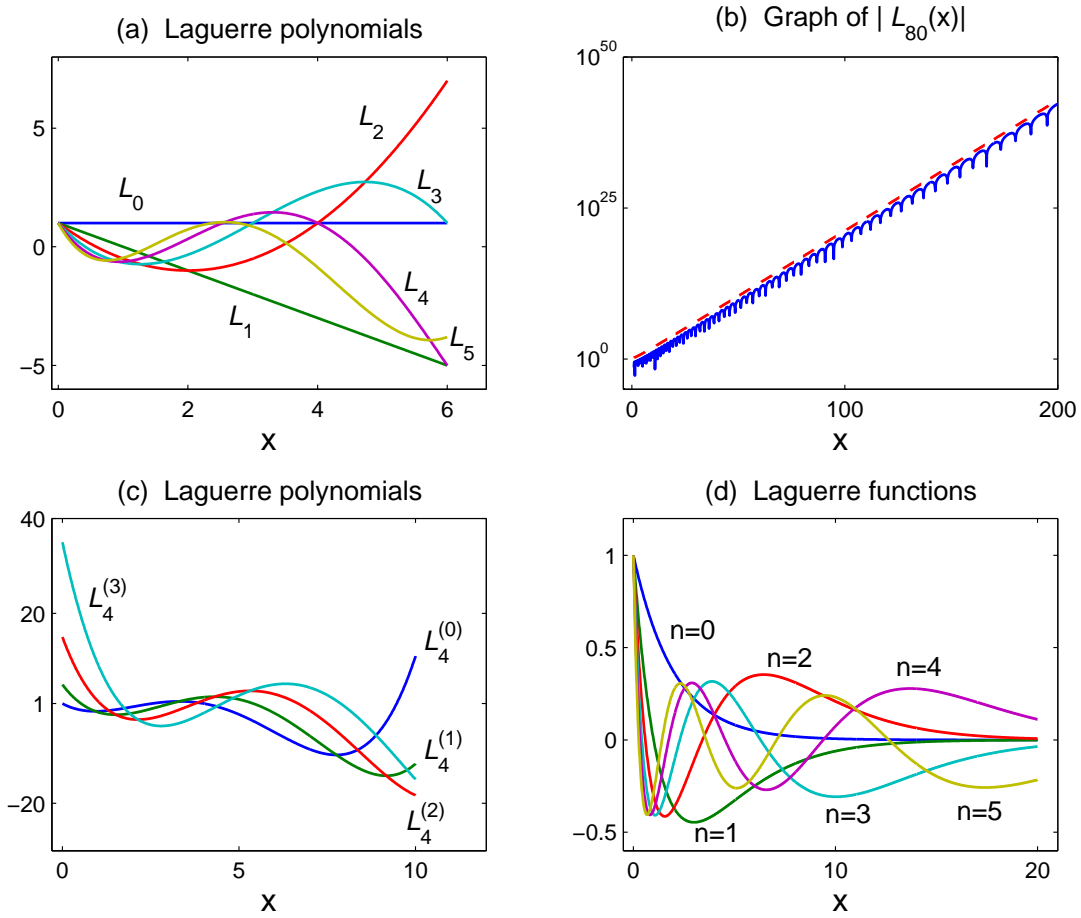


Figure 2: (a) Graphs of the first six Laguerre polynomials $\mathcal{L}_n(x)$ with $n=0,1,\dots,5$ and $x \in [0,6]$; (b) Growth of $|\mathcal{L}_{80}(x)|$ against the upper bound $x^{-1/4}e^{x/2}$ (dashed line); (c) Graphs of the generalized Laguerre polynomials $\mathcal{L}_4^{(\alpha)}(x)$ with $\alpha=0,1,2,3$ and $x \in [0,10]$; (d) Graphs of the first six Laguerre functions $\hat{\mathcal{L}}_n(x)$ with $n=0,1,\dots,5$ and $x \in [0,20]$.

3.1.4 Approximation results by generalized Laguerre functions

It is straightforward to extend the Laguerre polynomial approximations to the Laguerre function approximations. Indeed, for any $u \in L^2_{\hat{\omega}_\alpha}(\Lambda)$, we have $ue^{x/2} \in L^2_{\omega_\alpha}(\Lambda)$. Let us denote

$$\hat{P}_N := \{v : v = e^{-x/2}w \text{ with } w \in P_N\}, \tag{3.24}$$

and define the operator

$$\hat{\pi}_{N,\alpha} u = e^{-x/2} \pi_{N,\alpha}(ue^{x/2}) \in \hat{P}_N. \tag{3.25}$$

Clearly, by (3.6),

$$(\hat{\pi}_{N,\alpha} u - u, v_N)_{\hat{\omega}_\alpha} = (\pi_{N,\alpha}(ue^{x/2}) - (ue^{x/2}), (v_N e^{x/2}))_{\omega_\alpha} = 0, \quad \forall v_N \in \hat{P}_N. \tag{3.26}$$

Hence, $\hat{\pi}_{N,\alpha}$ is the orthogonal projector from $L^2_{\hat{\omega}_\alpha}(\Lambda)$ to \hat{P}_N , and therefore its approximation properties can be derived from that of $\pi_{N,\alpha}$.

Let $\hat{\partial}_x = \partial_x + 1/2$. We define

$$\hat{B}_\alpha^m(\Lambda) := \{u : \hat{\partial}_x^k u \in L^2_{\hat{\omega}_{\alpha+k}}(\Lambda), 0 \leq k \leq m\}, \quad (3.27)$$

equipped with the norm and semi-norm

$$\|u\|_{\hat{B}_\alpha^m} = \left(\sum_{k=0}^m \|\hat{\partial}_x^k u\|_{\hat{\omega}_{\alpha+k}}^2 \right)^{1/2}, \quad |u|_{\hat{B}_\alpha^m} = \|\hat{\partial}_x^m u\|_{\hat{\omega}_{\alpha+m}}.$$

Then, we have the following result for $\hat{\pi}_{N,\alpha}$.

Theorem 3.3. For any $\alpha > -1$ and $u \in \hat{B}_\alpha^m(\Lambda)$,

$$\|\hat{\partial}_x^l(\hat{\pi}_{N,\alpha}u - u)\|_{\hat{\omega}_{\alpha+l}} \lesssim N^{(l-m)/2} \|\hat{\partial}_x^m u\|_{\hat{\omega}_{\alpha+m}}. \quad (3.28)$$

Proof. Let $v = ue^{x/2}$. One verifies easily from (3.18) that

$$\partial_x^l(\pi_{N,\alpha}v - v) = \partial_x^l(e^{x/2}(\hat{\pi}_{N,\alpha}u - u)) = e^{x/2}\hat{\partial}_x^l(\hat{\pi}_{N,\alpha}u - u),$$

and likewise, $\partial_x^m v = e^{x/2}\hat{\partial}_x^m u$. Hence, the desired result is a direct consequence of (3.11). \square

Remark 3.1. When comparing the error estimate in the above theorem with the corresponding result for classical Jacobi approximation (see Lemma 2.1), we notice that the convergence rate of the Laguerre approximation is only half of the classical Jacobi approximation. This is a direct consequence of the linear growth of the eigenvalues in the Laguerre Sturm-Liouville problem, as opposed to the quadratic growth in the Jacobi Sturm-Liouville problem.

The comparison with the mapped Jacobi approximation (cf. Theorem 2.1) is more delicate.

Consider $u(x) = (1+x)^{-h}$ and $u(x) = \sin kx \cdot (1+x)^{-h}$. It can be easily checked that for both functions $\|\hat{\partial}_x^m u\|_{\hat{\omega}_{\alpha+m}} < \infty$ if $m < 2h - \alpha - 1$ which implies that

$$\|u - \hat{\pi}_{N,\alpha}u\|_{\hat{\omega}_\alpha} \lesssim N^{-(2h-\alpha-1)/2}. \quad (3.29)$$

Comparing with the error estimates by mapped Jacobi polynomials in (2.34) and (2.35), we observe that the mapped Jacobi approximation leads to better convergence rate for functions without oscillation at infinity such as $u(x) = (1+x)^{-h}$, but the Laguerre approximation is better for functions with oscillation at infinity such as $u(x) = \sin kx \cdot (1+x)^{-h}$.

Next, we define an orthogonal projector in $H_0^1(\Lambda)$ through the operator $\pi_N^{1,0}$. Since for any $u \in H_0^1(\Lambda)$, we have $ue^{x/2} \in H_{0,\omega}^1(\Lambda)$. Let us denote

$$\hat{P}_N^0 := \{v \in \hat{P}_N : u(0) = 0\}, \quad (3.30)$$

and define the operator

$$\hat{\pi}_N^{1,0}u = e^{-x/2}\pi_N^{1,0}(ue^{x/2}) \in \hat{P}_N^0.$$

The following results characterize the properties of $\pi_N^{1,0}$ (cf. [48]).

Theorem 3.4.

$$((u - \hat{\pi}_N^{1,0}u)', v'_N) + \frac{1}{4}(u - \hat{\pi}_N^{1,0}u, v_N) = 0, \quad \forall u \in H_0^1(\Lambda), v_N \in \hat{P}_N^0; \tag{3.31}$$

and for $m \geq 1$,

$$\|\hat{\pi}_N^{1,0}u - u\|_1 \lesssim N^{\frac{1}{2} - \frac{m}{2}} \|\hat{\partial}_x^m u\|_{\hat{\omega}_{m-1}}, \quad \forall u \in H_0^1(\Lambda) \text{ with } \hat{\partial}_x u \in \hat{B}_0^{m-1}(\Lambda). \tag{3.32}$$

Proof. Using the definition of $\pi_N^{1,0}$, and integration by parts, we find that for any $v_N = w_N e^{-x/2}$ with $w_N \in P_N^0$,

$$\begin{aligned} & ((u - \hat{\pi}_N^{1,0}u)', v'_N) \\ &= \left([(ue^{x/2}) - \pi_N^{1,0}(ue^{x/2})]' - \frac{1}{2}[(ue^{x/2}) - \pi_N^{1,0}(ue^{x/2})], w'_N - \frac{1}{2}w_N \right)_\omega \\ &= -\frac{1}{2} \int_0^\infty [(ue^{x/2}) - \pi_N^{1,0}(ue^{x/2})w_N]' e^{-x} dx + \frac{1}{4} ((ue^{x/2}) - \pi_N^{1,0}(ue^{x/2}), w_N)_\omega \\ &= -\frac{1}{4} ((ue^{x/2}) - \pi_N^{1,0}(ue^{x/2}), v_N)_\omega \\ &= -\frac{1}{4} (u - \hat{\pi}_N^{1,0}u, v_N), \end{aligned}$$

which implies the identity (3.31).

Now let $v = ue^{x/2}$. It is clear that

$$\partial_x(\hat{\pi}_N^{1,0}u - u) = -\frac{1}{2}e^{-x/2}(\pi_N^{1,0}v - v) + e^{-x/2}\partial_x(\pi_N^{1,0}v - v).$$

Hence, using Lemma 3.2 and the fact that $\partial_x^m v = e^{x/2}\hat{\partial}_x^m u$, leads to

$$\begin{aligned} \|\partial_x(\hat{\pi}_N^{1,0}u - u)\| &\lesssim \|\pi_N^{1,0}v - v\|_\omega + \|\partial_x(\pi_N^{1,0}v - v)\|_\omega \\ &\lesssim N^{\frac{1}{2} - \frac{m}{2}} \|x^{\frac{m-1}{2}} \partial_x^m v\|_\omega \lesssim N^{\frac{1}{2} - \frac{m}{2}} \|x^{\frac{m-1}{2}} \hat{\partial}_x^m u\|. \end{aligned}$$

Similarly, we have

$$\|\hat{\pi}_N^{1,0}u - u\| \lesssim N^{\frac{1}{2} - \frac{m}{2}} \|\hat{\partial}_x^m u\|_{\hat{\omega}_{m-1}}.$$

This completes the proof. □

3.2 Laguerre-Gauss type quadratures and interpolation by Laguerre polynomials/functions

We recall first the (generalized) Laguerre-Gauss type quadratures (cf. [19, 52]).

Theorem 3.5. Let $\{x_j^{(\alpha)}, \omega_j^{(\alpha)}\}_{j=0}^N$ be the nodes and weights associated with the Laguerre-Gauss or Laguerre-Gauss-Radau quadrature. Then,

$$\int_0^{+\infty} p(x)x^\alpha e^{-x} dx = \sum_{j=0}^N p(x_j^{(\alpha)})\omega_j^{(\alpha)}, \quad \forall p \in P_{2N+\delta}, \tag{3.33}$$

where $\delta = 1, 0$ for Laguerre-Gauss and Laguerre-Gauss-Radau quadrature, respectively.

- For the Laguerre-Gauss quadrature:

$$\begin{aligned} \{x_j^{(\alpha)}\}_{j=0}^N &\text{ are the zeros of } \mathcal{L}_{N+1}^{(\alpha)}(x); \\ \omega_j^{(\alpha)} &= -\frac{\Gamma(N+\alpha+1)}{(N+1)!} \frac{1}{\mathcal{L}_N^{(\alpha)}(x_j^{(\alpha)})\partial_x \mathcal{L}_{N+1}^{(\alpha)}(x_j^{(\alpha)})} \\ &= \frac{\Gamma(N+\alpha+1)}{(N+\alpha+1)(N+1)!} \frac{x_j^{(\alpha)}}{[\mathcal{L}_N^{(\alpha)}(x_j^{(\alpha)})]^2}, \quad 0 \leq j \leq N. \end{aligned} \tag{3.34}$$

- For the Laguerre-Gauss-Radau quadrature:

$$\begin{aligned} x_0^{(\alpha)} &= 0, \{x_j^{(\alpha)}\}_{j=1}^N \text{ are the zeros of } \partial_x \mathcal{L}_{N+1}^{(\alpha)}(x); \\ \omega_0^{(\alpha)} &= \frac{(\alpha+1)\Gamma^2(\alpha+1)\Gamma(N+1)}{\Gamma(N+\alpha+2)}, \\ \omega_j^{(\alpha)} &= \frac{\Gamma(N+\alpha+1)}{N!(N+\alpha+1)} \frac{1}{[\partial_x \mathcal{L}_N^{(\alpha)}(x_j^{(\alpha)})]^2} \\ &= \frac{\Gamma(N+\alpha+1)}{N!(N+\alpha+1)} \frac{1}{[\mathcal{L}_N^{(\alpha)}(x_j^{(\alpha)})]^2}, \quad 1 \leq j \leq N. \end{aligned} \tag{3.35}$$

In practice, the above quadrature is rarely used due to the exponential weight. Instead, the following quadratures with respect to the weight function $\hat{\omega}_\alpha$ should be used.

Theorem 3.6. Let $\{x_j^{(\alpha)}, \omega_j^{(\alpha)}\}$ be the set of Laguerre-Gauss or Laguerre-Gauss-Radau quadrature nodes and weights given in Theorem 3.5. Denote

$$\hat{\omega}_j^{(\alpha)} = e^{x_j^{(\alpha)}} \omega_j^{(\alpha)}, \quad 0 \leq j \leq N. \tag{3.36}$$

Then we have

$$\int_0^{+\infty} p(x)q(x)x^\alpha dx = \sum_{j=0}^N p(x_j^{(\alpha)})q(x_j^{(\alpha)})\hat{\omega}_j^{(\alpha)}, \quad \forall p, q \in \widehat{P}_{2N+\delta},$$

where $\delta = 1, 0$ for the Laguerre-Gauss case and Laguerre-Gauss-Radau case, respectively.

Remark 3.2. Thanks to the three-term recursive relation satisfied by the GLPs, the nodes for the Laguerre-Gauss and Laguerre-Gauss-Radau quadratures can be easily computed as eigenvalues of the symmetric tridiagonal matrix

$$A_{N+1} = \begin{bmatrix} a_0 & -\sqrt{b_1} & & & \\ -\sqrt{b_1} & a_1 & & & \\ & & \ddots & & \\ & & & -\sqrt{b_{N-1}} & a_{N-1} & -\sqrt{b_N} \\ & & & & -\sqrt{b_N} & a_N \end{bmatrix}, \quad (3.37)$$

whose entries are determined by (3.3):

$$a_j = 2j + \alpha + 1, \quad 0 \leq j \leq N, \quad b_j = j(j + \alpha), \quad 1 \leq j \leq N. \quad (3.38)$$

However, care should be taken when computing the weights $\{\hat{\omega}_j^{(\alpha)}\}$. The process of computing first $\{\omega_j^{(\alpha)}\}$ and then using (3.36) is highly ill-conditioned and should be avoided. Instead, thanks to (3.15) and (3.36), we derive easily that for the Laguerre-Gauss case, we have

$$\hat{\omega}_j^{(\alpha)} = \frac{\Gamma(N + \alpha + 1)}{(N + \alpha + 1)(N + 1)!} \frac{x_j^{(\alpha)}}{[\hat{\mathcal{L}}_N^{(\alpha)}(x_j^{(\alpha)})]^2}, \quad (3.39)$$

and for the Laguerre-Gauss-Radau case (with $x_0^{(\alpha)} = 0$), we have

$$\hat{\omega}_0^{(\alpha)} = \omega_0^{(\alpha)}; \quad \hat{\omega}_j^{(\alpha)} = \frac{\Gamma(N + \alpha + 1)}{N!(N + \alpha + 1)} \frac{1}{[\hat{\mathcal{L}}_N^{(\alpha)}(x_j^{(\alpha)})]^2}, \quad j \geq 1. \quad (3.40)$$

We now examine the distributions of the quadratures nodes with respect to N and the parameter α . We first recall two formulas in Szegő [52]. Assuming that the zeros $\{x_j^{(\alpha)}\}_{j=0}^N$ of $\mathcal{L}_{N+1}^{(\alpha)}(x)$ are arranged in ascending order, we have the following properties

$$x_0^{(\alpha)} > \frac{c}{N+1}, \quad x_N^{(\alpha)} = 4(N+1) + 2\alpha + 2 - c(4N+4)^{1/3}, \quad (3.41a)$$

$$x_j^{(\alpha)} \sim \frac{(j+1)^2}{N+1}, \quad 0 \leq j \leq N, \quad (3.41b)$$

where c is a positive constant independent of N . Hence, the largest zero grows like $4N$, while the smallest zero behaves like $\mathcal{O}(N^{-1})$. Such properties can be visualized from Fig. 3(a)-(c). Indeed, we observe from Fig. 3(a) and (b) that the nodes are clustered near the endpoint $x = 0$, with a density

$$\min_j |x_{j+1} - x_j| \sim N^{-1}$$

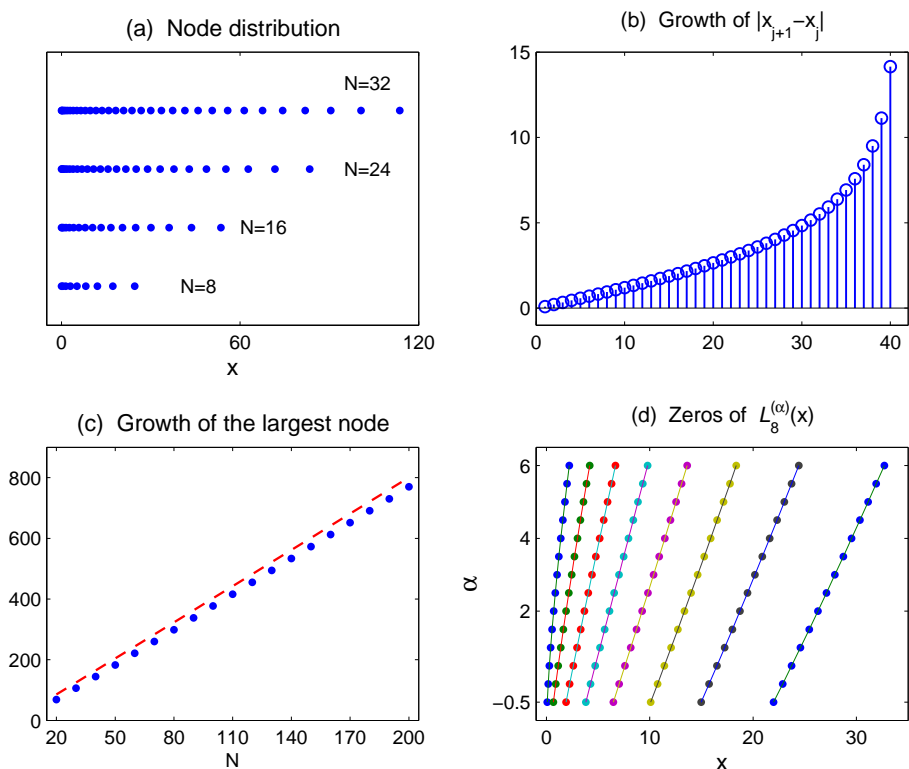


Figure 3: (a) Distribution of Laguerre-Gauss-Radau nodes $\{x_j\}_{j=0}^N$ with $N=8,16,24,32$ with $\alpha=0$; (b) Growth of $\{|x_{j+1}-x_j|\}_{j=0}^{40}$; (c) Growth of the largest node x_N against the asymptotic estimate: $4(N+1)+2-(4(N+1))^{1/3}$ (cf. (3.41a)) with various N ; (d) Distribution of zeros of $L_8^{(\alpha)}(x)$ with various α .

as opposed to the $\mathcal{O}(N^{-2})$ behavior in the mapped Jacobi case. Fig. 3(c) shows that the largest node x_N grows at the rate $4(N+1)+2-(4(N+1))^{1/3}$ as N increases. Another interesting property which can be visualized from Fig. 3(d) is that for fixed N and j , $x_j^{(\alpha)}$ increases as α increases, i.e., we have

$$\frac{\partial x_j^{(\alpha)}}{\partial \alpha} > 0, \quad \text{for } 0 \leq j \leq N. \tag{3.42}$$

Let $\{x_j^{(\alpha)}\}_{j=0}^N$ be the Laguerre-Gauss or Gauss-Radau interpolation nodes defined in Theorem 3.5, and denote by $I_N^{(\alpha)}$ the interpolation operator from $C(\bar{\Lambda})$ onto P_N based on the set $\{x_j^{(\alpha)}\}_{j=0}^N$. We have the following result (cf. [27]):

Theorem 3.7. *Assuming $u \in C(\bar{\Lambda})$, $u \in B_\alpha^m(\Lambda)$ and $\partial_x u \in B_\alpha^{m-1}(\Lambda)$ with $m \geq 1$, then*

$$\|I_N^{(\alpha)} u - u\|_{\omega_\alpha} \lesssim N^{(1-m)/2} \left(\|\partial_x^m u\|_{\omega_{\alpha+m-1}} + (\ln N)^{1/2} \|\partial_x^m u\|_{\omega_{\alpha+m}} \right).$$

Remark 3.3. Compared with Theorem 3.1 (with $l = 0$), the estimate for the interpolation is suboptimal (with order $\mathcal{O}(N^{(1-m)/2} \ln N)$). The above result is proved in [27] and improves previous results in [42, 43, 58]. In [42] (see also [6]), the following estimate was derived for the case $\alpha = 0$,

$$\|I_N^{(0)} u - u\|_{\omega_0} \lesssim N^{(1-m)/2} \|u\|_{m, \omega_\tau}, \tag{3.43}$$

where the weight function $\omega_\tau(x) = e^{-(1-\tau)x}$ with $0 < \tau < 1$. Mastroianni and Occorsio [43] studied the generalized Laguerre-Gauss interpolation (see Formula (3.8) of [43]) and showed that

$$\|x^\gamma e^{-x/2} (I_N^{(\alpha)} u - u)\|_{L^\infty} \lesssim N^{-m/2} \ln N \|x^{m/2+\gamma} e^{-x/2} \partial_x^m u\|_{L^\infty}, \tag{3.44}$$

for $m \geq 1, \alpha > -1$ and some $\gamma \geq 0$ satisfying

$$2\gamma - \frac{5}{2} \leq \alpha \leq 2\gamma - \frac{1}{2}.$$

In [58], the usual Laguerre interpolation was analyzed in the weighted Sobolev space, and the main result is

$$\|I_N^{(0)} u - u\|_{\omega_0} \lesssim N^{(1-m)/2+\varepsilon} \|u\|_{m, \omega_m}, \quad m \geq 1, \quad 0 < \varepsilon \leq \frac{1}{2}. \tag{3.45}$$

This result was improved in [27] with $\ln N$ in place of N^ε .

We now define the interpolation operator $\hat{I}_N^{(\alpha)}$ from $C(\bar{\Lambda})$ onto \hat{P}_N based on the set of points $\{x_j^{(\alpha)}\}_{j=0}^N$ i.e.,

$$(\hat{I}_N^{(\alpha)} u)(x_j^{(\alpha)}) = u(x_j^{(\alpha)}), \quad 0 \leq j \leq N.$$

By observing that

$$(\hat{I}_N^{(\alpha)} u)(x) = e^{-x/2} I_N^{(\alpha)} (ue^{x/2}) \in \hat{P}_N,$$

we derive immediately from Theorem 3.7 the following result.

Theorem 3.8. Let $\hat{\partial}_x = \partial_x + \frac{1}{2}$. Assuming $u \in C(\bar{\Lambda}), u \in \hat{B}_\alpha^m(\Lambda)$ and $\hat{\partial}_x u \in \hat{B}_\alpha^{m-1}(\Lambda)$ with $m \geq 1$, we have

$$\|\hat{I}_N^{(\alpha)} u - u\|_{\hat{\omega}_\alpha} \lesssim N^{(1-m)/2} (\|\hat{\partial}_x^m u\|_{\hat{\omega}_{\alpha+m-1}} + (\ln N)^{1/2} \|\hat{\partial}_x^m u\|_{\hat{\omega}_{\alpha+m}}).$$

3.3 Numerical methods using Laguerre functions

We consider again the model problem (2.51). An advantage of using Laguerre functions is that they are mutually orthogonal in the usual (non-weighted) L^2 space so we can work with the usual (i.e., non-weighted) variational formulation.

Let us denote

$$H_0^1(\Lambda) = \{u \in H^1(\Lambda) : u(0) = 0\}. \tag{3.46}$$

Then, a weak formulation for (2.51) is to find $u \in H_0^1(\Lambda)$ such that

$$a(u, v) := \gamma(u, v) + (u', v') = (f, v), \quad \forall v \in H_0^1(\Lambda), \quad (3.47)$$

for $f \in (H_0^1(\Lambda))'$. We note that $u \in H_0^1(\Lambda)$ indicates a decay condition: $\lim_{x \rightarrow +\infty} u(x) = 0$.

The Laguerre-spectral approximation to (3.47) is to find $u_N \in \widehat{P}_N^0$ such that

$$a(u_N, v_N) = (\widehat{I}_N f, v_N), \quad \forall v_N \in \widehat{P}_N^0, \quad (3.48)$$

where \widehat{P}_N^0 is defined in (3.30) and $\widehat{I}_N = \widehat{I}_N^{(\alpha)}$ with $\alpha = 0$.

It is clear that for $\gamma > 0$, the problem admits a unique solution, since

$$a(u, u) = |u|_1^2 + \gamma \|u\|^2 \geq \min(1, \gamma) \|u|_1|^2, \quad \text{for all } u \in H_0^1(\Lambda).$$

Theorem 3.9. *Let $\gamma > 0$, $u \in H_0^1(\Lambda)$, $\hat{\partial}_x u \in \widehat{B}_0^{m-1}(\Lambda)$, $f \in C(\bar{\Lambda}) \cap \widehat{B}_0^k(\Lambda)$ and $\hat{\partial}_x f \in \widehat{B}_0^{k-1}(\Lambda)$ with $k, m \geq 1$. Then,*

$$\|u - u_N\|_1 \lesssim N^{\frac{1}{2} - \frac{m}{2}} \|\hat{\partial}_x^m u\|_{\widehat{\omega}_{m-1}} + N^{(1-k)/2} (\|\hat{\partial}_x^k f\|_{\widehat{\omega}_{k-1}} + (\ln N)^{1/2} \|\hat{\partial}_x^k f\|_{\widehat{\omega}_k}). \quad (3.49)$$

Proof. Let $e_N = u_N - \widehat{\pi}_N^{1,0} u$ and $\tilde{e}_N = u - \widehat{\pi}_N^{1,0} u$. Hence, by (3.47)–(3.48),

$$a(u_N - u, v_N) = (\widehat{I}_N f - f, v_N), \quad \forall v_N \in \widehat{P}_N^0,$$

which implies that

$$a(e_N, v_N) = a(\tilde{e}_N, v_N) + (\widehat{I}_N f - f, v_N), \quad \forall v_N \in \widehat{P}_N^0.$$

Taking $v_N = e_N$ in the above, we find

$$\|e_N\|_1 \lesssim \|\tilde{e}_N\|_1 + \|\widehat{I}_N f - f\|_0.$$

We can then conclude by using Theorems 3.4 and 3.7 and the triangular inequality. \square

Remark 3.4. In [47], numerical results are reported for the scheme (3.48) using the functions in (2.31)–(2.33) as exact solutions. Geometric convergence rates (i.e., $\exp(-cN)$) for (2.31) and sub-geometric convergence of order $\exp(-c\sqrt{N})$ for (2.32) are observed (cf. Fig. 3.2 in [47]), while a convergence rate consistent with the estimate in (3.49) and (3.29) is observed for (2.33). The sub-geometric convergence for (2.32) was puzzling since the error estimate in (3.29) only predicts a rate of order about N^{-h} . In order to explain this surprising disagreement, we performed additional tests with different h and with N much larger than what was used in [47]. The numerical results are reported in Fig. 4. On the left, we plot the results with $h = 3$ and 4.5 for N up to 128, and we observe again the sub-geometric convergence rate as reported in [47]. However, when we increased N further, the convergence rates eventually became algebraic. This indicates that the sub-geometric convergence reported in [47] was still in the pre-asymptotic range. To illustrate this behavior, we plot the results with $h = 1.5$ and 2 (so the asymptotic range can be reached faster) for N up to 256 on the right of Fig. 4. It is clear that after a pre-asymptotic range, the convergence rates settle down to the algebraic rates consistent with (3.49) and (3.29).

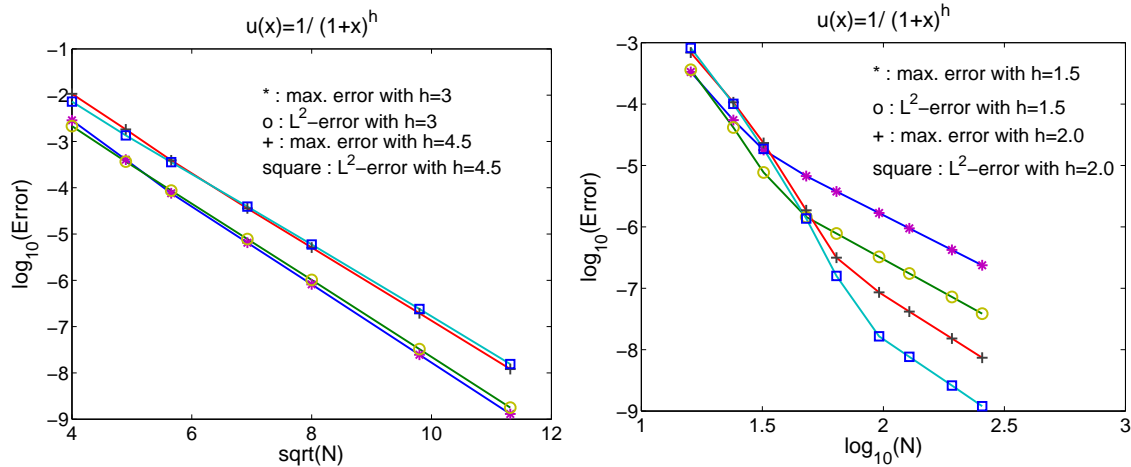


Figure 4: Convergence rates of the scheme (3.48).

4 Hermite spectral methods

For problems in the whole line, a natural choice is to use Hermite polynomials/functions.

4.1 Approximations by Hermite polynomials/functions

We first recall some basic properties of Hermite polynomials/functions.

4.1.1 Hermite polynomials

The Hermite polynomials, denoted by $H_n(x)$, are the eigenfunctions of the Sturm-Liouville problem:

$$e^{x^2} (e^{-x^2} H'_n(x))' + \lambda_n H_n(x) = 0, \quad \forall x \in \mathcal{R} := (-\infty, \infty), \quad (4.1)$$

with the eigenvalue $\lambda_n = 2n$ grows linearly with respect to n .

The Hermite polynomials are orthogonal with respect to the weight $\omega(x) = e^{-x^2}$, i.e.,

$$\int_{-\infty}^{+\infty} H_m(x) H_n(x) e^{-x^2} dx = \gamma_n \delta_{mn}, \quad \gamma_n = \sqrt{\pi} 2^n n!. \quad (4.2)$$

Note that the constant γ_n grows exponentially as n increases, so it is necessary to normalize this factor in actual computations.

The three-term recurrence formula reads

$$H_{n+1}(x) = 2xH_n(x) - 2nH_{n-1}(x), \quad n \geq 1. \quad (4.3)$$

As a direct consequence of (4.1) and (4.2), we have the orthogonality:

$$\int_{-\infty}^{\infty} H'_n(x) H'_m(x) e^{-x^2} dx = \lambda_n \gamma_n \delta_{mn}. \quad (4.4)$$

The Hermite polynomials satisfy the recurrence relations:

$$H'_n(x) = 2nH_{n-1}(x), \quad n \geq 1, \quad (4.5a)$$

$$H'_n(x) = 2xH_n(x) - H_{n+1}(x), \quad n \geq 0. \quad (4.5b)$$

4.1.2 Approximations by Hermite polynomials

Consider the L^2_ω -orthogonal projection $\pi_N: L^2_\omega(\mathcal{R}) \rightarrow P_N$, defined by

$$(u - \pi_N u, v_N)_\omega = 0, \quad \forall v_N \in P_N.$$

Similar to Theorem 3.1, we have the following result.

Theorem 4.1. For any $u \in H^m_\omega(\mathcal{R})$ with $m \geq 0$,

$$\|\partial_x^k(\pi_N u - u)\|_\omega \lesssim N^{(k-m)/2} \|\partial_x^m u\|_\omega, \quad 0 \leq k \leq m. \quad (4.6)$$

Proof. For any $u \in L^2_\omega(\mathcal{R})$, we write the Hermite expansion

$$u(x) = \sum_{n=0}^{\infty} \tilde{u}_n H_n(x) \quad \text{with} \quad \tilde{u}_n = \frac{1}{\sqrt{\pi} 2^n n!} \int_{-\infty}^{\infty} u(x) H_n(x) e^{-x^2} dx.$$

We derive from (4.5a) that

$$\partial_x^k H_n(x) = 2^k n(n-1)\cdots(n-k+1) H_{n-k}(x) := \sigma_n^k H_{n-k}(x), \quad n \geq k. \quad (4.7)$$

Therefore, for $k \leq m \leq N$,

$$\begin{aligned} \|\partial_x^k(\pi_N u - u)\|_\omega^2 &= \left\| \sum_{n=N+1}^{\infty} \tilde{u}_n \partial_x^k H_n(x) \right\|_\omega^2 \\ &= \sum_{n=N+1}^{\infty} \tilde{u}_n^2 (\sigma_n^k)^2 \gamma_{n-k} = \sum_{n=N+1}^{\infty} \tilde{u}_n^2 \frac{(\sigma_n^k)^2 \gamma_{n-k}}{(\sigma_n^m)^2 \gamma_{n-m}} (\sigma_n^m)^2 \gamma_{n-m} \\ &\lesssim N^{k-m} \sum_{n=N+1}^{\infty} \tilde{u}_n^2 (\sigma_n^m)^2 \gamma_{n-m} = N^{k-m} \|\partial_x^m u\|_\omega^2. \end{aligned}$$

This completes the proof. □

4.1.3 Hermite functions

As the (generalized) Laguerre polynomials, the Hermite polynomials are generally not suitable in practice due to their wild asymptotic behavior at infinities (cf. [52]):

$$\begin{aligned} H_n(x) &\sim \frac{\Gamma(n+1)}{\Gamma(n/2+1)} e^{x^2/2} \cos\left(\sqrt{2n+1}x - \frac{n\pi}{2}\right) \\ &\sim n^{n/2} e^{x^2/2} \cos\left(\sqrt{2n+1}x - \frac{n\pi}{2}\right). \end{aligned} \quad (4.8)$$

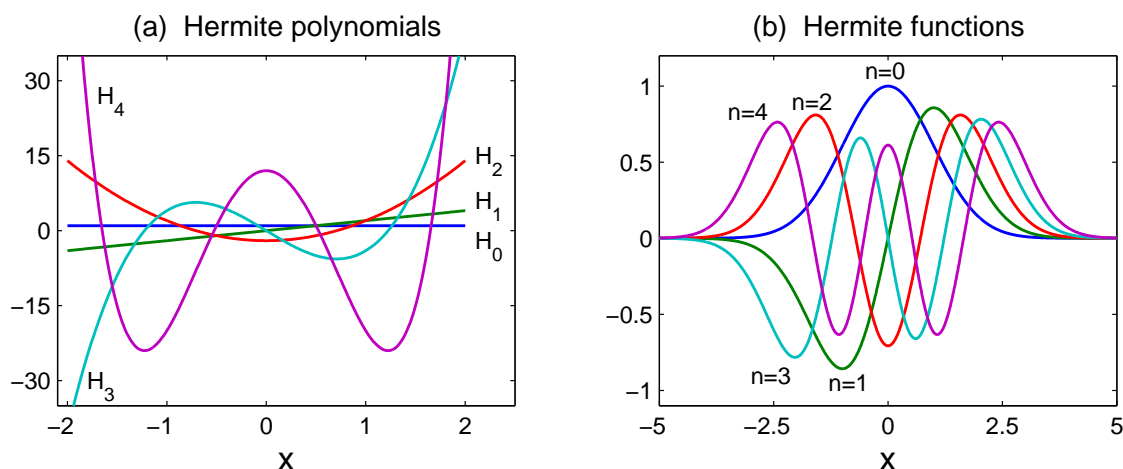


Figure 5: (a) The first five Hermite polynomials $H_n(x)$ with $n=0, \dots, 4$; (b) The first five Hermite functions $\tilde{H}_n(x)$ with $n=0, \dots, 4$.

Hence, we shall consider the so called Hermite functions.

The normalized Hermite function of degree n is defined by

$$\tilde{H}_n(x) = \frac{1}{\sqrt{2^n n!}} e^{-x^2/2} H_n(x), \quad n \geq 0, x \in \mathcal{R}. \tag{4.9}$$

Clearly, $\{\tilde{H}_n\}$ is an orthogonal system in $L^2(\mathcal{R})$, i.e.,

$$\int_{-\infty}^{+\infty} \tilde{H}_n(x) \tilde{H}_m(x) dx = \sqrt{\pi} \delta_{mn}. \tag{4.10}$$

In contrast to the Hermite polynomials, the Hermite functions are well behaved with the decay property:

$$|\tilde{H}_n(x)| \rightarrow 0, \quad \text{as } |x| \rightarrow \infty,$$

and the asymptotic formula with large n is

$$\tilde{H}_n(x) \sim n^{-\frac{1}{4}} \cos\left(\sqrt{2n+1}x - \frac{n\pi}{2}\right). \tag{4.11}$$

Some sample graphs of the Hermite polynomials and the normalized Hermite functions are presented in Fig. 5.

The three-term recurrence relation (4.3) implies

$$\begin{aligned} \tilde{H}_{n+1}(x) &= x \sqrt{\frac{2}{n+1}} \tilde{H}_n(x) - \sqrt{\frac{n}{n+1}} \tilde{H}_{n-1}(x), \quad n \geq 1, \\ \tilde{H}_0(x) &= e^{-x^2/2}, \quad \tilde{H}_1(x) = \sqrt{2}x e^{-x^2/2}. \end{aligned} \tag{4.12}$$

Using (4.5a) and the above formula leads to

$$\begin{aligned} \tilde{H}'_n(x) &= \sqrt{2n}\tilde{H}_{n-1}(x) - x\tilde{H}_n(x) \\ &= \sqrt{\frac{n}{2}}\tilde{H}_{n-1}(x) - \sqrt{\frac{n+1}{2}}\tilde{H}_{n+1}(x). \end{aligned} \tag{4.13}$$

4.1.4 Approximations by Hermite functions

Let us define $\tilde{P}_N = \{v : v = e^{-x^2/2}w, w \in P_N\}$. Since $ue^{x^2/2} \in L^2_\omega(\mathcal{R})$ for any $u \in L^2(\mathcal{R})$, we define $\tilde{\pi}_N : L^2(\mathcal{R}) \rightarrow \tilde{P}_N$ by

$$\tilde{\pi}_N u := e^{-x^2/2}\pi_N(ue^{x^2/2}) \in \tilde{P}_N. \tag{4.14}$$

Therefore,

$$(u - \tilde{\pi}_N u, v_N) = (ue^{x^2/2} - \tilde{\pi}_N(ue^{x^2/2}), v_N e^{x^2/2})_\omega = 0, \quad \forall v_N \in \tilde{P}_N, \tag{4.15}$$

which implies that $\tilde{\pi}_N$ is in fact the orthogonal projection in $L^2(\mathcal{R})$. We introduce the derivative operator

$$\tilde{\partial}_x = \partial_x + x \text{ so that } \partial_x H_n(x) = e^{x^2/2}\tilde{\partial}_x \tilde{H}_n(x). \tag{4.16}$$

Then, it is straightforward to derive the following result from Theorem 4.1.

Theorem 4.2. For any $\tilde{\partial}_x^m u \in L^2(\mathcal{R})$ with $m \geq 0$,

$$\|\tilde{\partial}_x^l(\tilde{\pi}_N u - u)\| \lesssim N^{(l-m)/2} \|\tilde{\partial}_x^m u\|, \quad 0 \leq l \leq m. \tag{4.17}$$

A particularly interesting result for the Hermite case is the following theorem which shows that $\tilde{\pi}_N$ is simultaneously the optimal projector from $H^l(\mathcal{R}) \rightarrow \tilde{P}_N$ for $l=0,1,2$.

Theorem 4.3. For any $\tilde{\partial}_x^m u \in L^2(\mathcal{R})$ with $m \geq 0$,

$$\|\partial_x^l(\tilde{\pi}_N u - u)\| \lesssim N^{(l-m)/2} \|\partial_x^m u\|, \quad l=0,1,2, \quad l \leq m. \tag{4.18}$$

Proof. The case $l=0$ comes directly from Corollary 4.2 with $l=0$.

In case of $l=1$, note that

$$\begin{aligned} \partial_x(\tilde{\pi}_N u - u) &= e^{-x^2/2}\partial_x\left(\pi_N(e^{x^2/2}u) - (e^{x^2/2}u)\right) \\ &\quad - xe^{-x^2/2}\left(\pi_N(e^{x^2/2}u) - (e^{x^2/2}u)\right). \end{aligned}$$

Hence, by using the inequality (cf. [30])

$$\|xv\|_\omega \leq \|v\|_{1,\omega}, \tag{4.19}$$

and Theorem 4.1,

$$\begin{aligned} \|\partial_x(\tilde{\pi}_N u - u)\| &\leq \|\pi_N(e^{x^2/2}u) - (e^{x^2/2}u)\|_{1,\omega} + \|x(\pi_N(e^{x^2/2}u) - (e^{x^2/2}u))\|_\omega \\ &\lesssim \|\pi_N(e^{x^2/2}u) - (e^{x^2/2}u)\|_{1,\omega} \leq N^{1/2-m/2} \|\partial_x^m(e^{x^2/2}u)\|_\omega. \end{aligned}$$

The case $l=2$ can be proved in the same fashion. □

Remark 4.1. As in the Laguerre case, the eigenvalues of the Sturm-Liouville problem associated with the Hermite polynomials also grows linearly, so the convergence rate of the Hermite approximation is similar to that of the Laguerre approximation.

To compare with the mapped Jacobi approximation (cf. Theorem 2.1), we consider $u(x) = (1+x^2)^{-h}$ and $u(x) = \sin kx \cdot (1+x^2)^{-h}$. It can be checked that for both functions $\|\tilde{\partial}_x^m u\| < \infty$ if $m < \frac{4h-1}{2}$ which implies that

$$\|u - \tilde{\pi}_N u\| \lesssim N^{-(h-1/4)}. \tag{4.20}$$

Comparing with the error estimates by mapped Jacobi polynomials in (2.36) and (2.37), we observe that the mapped Jacobi approximation leads to better convergence rates for both functions.

4.2 Hermit Gauss quadrature and interpolation by Hermite polynomials/ functions

We start with the classical Hermite-Gauss quadrature with respect to the measure $e^{-x^2} dx$ (cf. [16]).

Theorem 4.4. Let $\{x_j, \omega_j\}_{j=0}^N$ be the Hermite-Gauss nodes and weights. Then, $\{x_j\}_{j=0}^N$ are the zeros of the Hermite polynomial $H_{N+1}(x)$,

$$\omega_j = \frac{\sqrt{\pi} 2^N N!}{(N+1) H_N^2(x_j)}, \quad 0 \leq j \leq N, \tag{4.21}$$

and we have

$$\int_{-\infty}^{\infty} p(x) e^{-x^2} dx = \sum_{j=0}^N p(x_j) \omega_j, \quad \forall p \in P_{2N+1}. \tag{4.22}$$

In practice, it is more convenient to use a quadrature rule relative to the measure dx and Hermite functions.

Theorem 4.5. Let $\{x_j, \omega_j\}_{j=0}^N$ be the Hermite-Gauss nodes and weights (cf. Theorem 4.4). We set

$$\tilde{\omega}_j = e^{x_j^2} \omega_j = \frac{\sqrt{\pi}}{(N+1) \tilde{H}_N^2(x_j)}, \quad 0 \leq j \leq N. \tag{4.23}$$

Then, we have

$$\int_{-\infty}^{\infty} p(x) q(x) dx = \sum_{j=0}^N p(x_j) q(x_j) \tilde{\omega}_j, \quad \forall p, q \in \tilde{P}_{2N+1}. \tag{4.24}$$

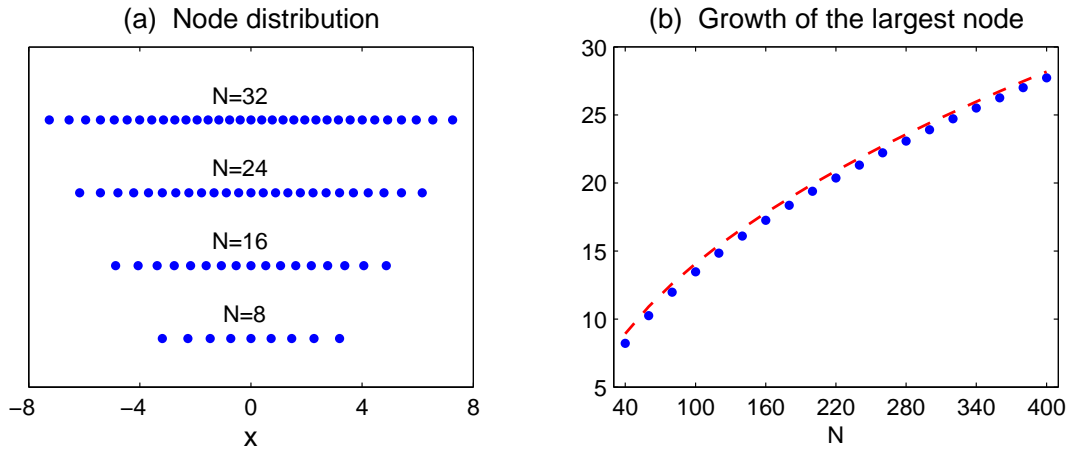


Figure 6: (a) Distribution of the Hermite-Gauss nodes $\{x_j\}_{j=0}^N$ with $N=8,16,24,32$; (b) Growth of the largest node against the asymptotic estimate: $\sqrt{2(N+1)} - (2(N+1))^{1/3}$ (dashed line) with various N .

Remark 4.2. As in the Laguerre case, the Hermite-Gauss nodes can be easily computed from the eigenvalues of a symmetric tridiagonal matrix

$$A_{N+1} = \begin{bmatrix} a_0 & \sqrt{b_1} & & & \\ \sqrt{b_1} & a_1 & \sqrt{b_2} & & \\ & \ddots & \ddots & \ddots & \\ & & \sqrt{b_{N-1}} & a_{N-1} & \sqrt{b_N} \\ & & & \sqrt{b_N} & a_N \end{bmatrix}, \tag{4.25}$$

whose entries are determined by (4.3):

$$a_j = 0, \quad 0 \leq j \leq N; \quad b_j = \frac{j}{2}, \quad 1 \leq j \leq N. \tag{4.26}$$

The weights $\{\tilde{\omega}_j\}_{j=0}^N$ can also be computed in a stable fashion by using (4.12) and (4.23).

In Fig. 6, we plot sample Hermite-Gauss nodes and the growth of the largest nodes with respect to N .

We now examine the interpolation errors. We start with the interpolation operator associated with the Hermite polynomials $I_N : C(\mathcal{R}) \rightarrow P_N$ such that $(I_N u)(x_j) = u(x_j)$, $0 \leq j \leq N$. By combining Theorem 4.1 and the results in [1, 29], we can prove the following result which is just a more concise form of Theorem 2.1 in [1, 29].

Theorem 4.6. For $u \in H_\omega^m(\mathcal{R})$ with $m \geq 1$, we have

$$\|\partial_x^l (I_N u - u)\|_\omega \lesssim N^{\frac{1}{6} + \frac{l-m}{2}} \|\partial_x^m u\|_\omega, \quad 0 \leq l \leq m.$$

We point out that [29] derived an order $N^{\frac{1}{3} + \frac{l-m}{2}}$, which was improved to $N^{\frac{1}{6} + \frac{l-m}{2}}$ by [1].

Next we define the interpolation operator associated with the Hermite function: $\tilde{I}_N : C(\mathcal{R}) \rightarrow \tilde{P}_N$ such that $(\tilde{I}_N u)(x_j) = u(x_j)$, $0 \leq j \leq N$.

By using the fact that $(\tilde{I}_N u) = e^{-x^2/2} I_N(ue^{x^2/2})$, we derive immediately from Theorem 4.6 the following result which is just a more concise form of Theorem 3.1 in [1, 36].

Theorem 4.7. For $u \in C(\mathcal{R})$ with $\tilde{\partial}_x^m u \in L^2(\mathcal{R})$ ($m \geq 1$), we have

$$\|\tilde{\partial}_x^l (\tilde{I}_N u - u)\| \lesssim N^{\frac{1}{6} + \frac{l-m}{2}} \|\tilde{\partial}_x^m u\|, \quad 0 \leq l \leq m.$$

Remark 4.3. The above interpolation results are not optimal in the sense that a factor of $N^{-1/6}$ is lost when compared with the best approximation error. It is an open question whether the factor $N^{1/6}$ can be removed from these estimates.

4.3 Numerical methods using Hermite functions

As an example of applications, we consider the following model problem:

$$-u_{xx} + \gamma u = f, \quad u(x) \rightarrow 0, \text{ as } |x| \rightarrow \infty. \tag{4.27}$$

A weak formulation for (4.27) is to find $u \in H^1(\mathcal{R})$ such that

$$(\partial_x u, \partial_x v) + \gamma(u, v) = (f, v), \quad \forall v \in H^1(\mathcal{R}), \tag{4.28}$$

for given $f \in (H^1(\mathcal{R}))'$, and the Hermite-Galerkin method for (4.28) is to find $u \in \tilde{P}_N$ such that

$$(\partial_x u_N, \partial_x v_N) + \gamma(u_N, v_N) = (\tilde{I}_N f, v_N), \quad \forall v_N \in \tilde{P}_N. \tag{4.29}$$

The following error estimate is a straightforward consequence of Theorems 4.3 and 4.7.

Theorem 4.8. If $u \in H^1(\mathcal{R})$ with $\tilde{\partial}_x^m u \in L^2(\mathcal{R})$, and $f \in C(\mathcal{R})$ with $\tilde{\partial}_x^k f \in L^2(\mathcal{R})$ ($k, m \geq 1$), we have

$$\|u_N - u\|_1 \lesssim N^{\frac{1-m}{2}} \|\tilde{\partial}_x^m u\| + N^{\frac{1}{3} - \frac{k}{2}} \|\tilde{\partial}_x^k f\|. \tag{4.30}$$

We now present numerical results using the scheme (4.29) with the exact solutions in (2.31)-(2.33) as exact solutions. On the left of Fig. 7, we observe a geometric convergence for (2.31). For (2.32), we observe essentially the same behavior as in the Laguerre case (cf. the right of Fig. 4), i.e., there is a pre-asymptotic range where one observes a sub-geometric convergence, but after the pre-asymptotic range, the convergence rates become algebraic as predicted in (4.20) and (4.30) (cf. the right of Fig. 7).

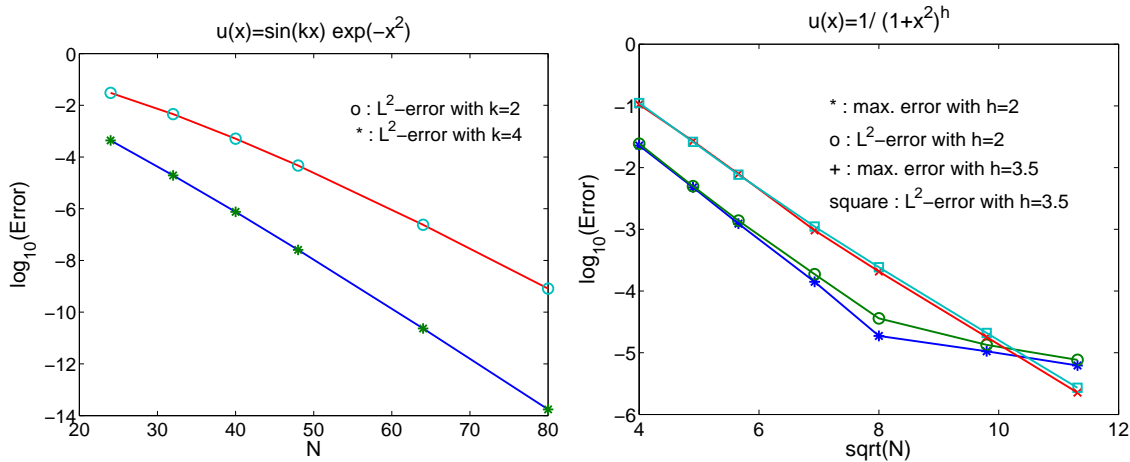


Figure 7: Convergence rates of the scheme (4.29).

5 Implementations, numerical results and discussions

5.1 Some implementation details

We start by saying that, given an approximation space X_N and a set of collocation points $\{x_j\}_{j=0}^N$, a collocation approach can be easily implemented. Indeed, let $\{h_j(x)\}_{j=0}^N \subseteq X_N$ be the Lagrange functions based on $\{x_j\}_{j=0}^N$, i.e., $h_j(x_i) = \delta_{ij}$. Then, as demonstrated in Section 2.5, we only need to know the derivative matrix $D = (D_{ij})$ where $D_{ij} = h_j'(x_i)$. Explicit formulas for classical orthogonal polynomials (Jacobi, Laguerre and Hermite) can be found in [19], and MATLAB codes for generating the derivative matrix is also available (cf. [56]). From these formulas, one can easily derive the corresponding formulas for mapped Jacobi polynomials, Laguerre and Hermite functions.

However, it is often more efficient and stable to use a Galerkin approach, particularly for problems with constant or polynomial coefficients and with large numbers of unknowns (cf. [46, 47]). We now briefly discuss how the Galerkin method presented in previous sections can be efficiently implemented.

Let X_N be the approximation space and ω be the weight function. The spectral-Galerkin method for the second-order model problems (2.51) or (4.27) can all be casted in the following form: Find $u_N \in X_N$ such that

$$\gamma(u_N, v_N)_\omega + (\partial_x u_N, \partial_x(v_N \omega)) = (I_N f, v_N)_\omega, \quad \forall v_N \in X_N, \quad (5.1)$$

where I_N is the corresponding interpolation operator.

Let $\{\phi_j\}_{j=0}^{N-1}$ be a set of basis functions for X_N . We denote

$$\begin{aligned}
 u_N &= \sum_{k=0}^{N-1} \hat{u}_k \phi_k(x), \quad \mathbf{u} = (\hat{u}_0, \hat{u}_1, \dots, \hat{u}_{N-1})^T, \\
 f_i &= (I_N f, \phi_i)_\omega, \quad \mathbf{f} = (f_0, f_1, \dots, f_{N-1})^T, \\
 s_{ik} &= (\phi'_k, (\phi_i \omega)'), \quad S = (s_{ik})_{0 \leq i, k \leq N-1}, \\
 m_{ik} &= (\phi_k, \phi_i)_\omega, \quad M = (m_{ik})_{0 \leq i, k \leq N-1}.
 \end{aligned}$$

Thus, the system (5.1) is reduced to the following matrix form

$$(\gamma M + S) \mathbf{u} = \mathbf{f}. \tag{5.2}$$

We now present suitable basis functions and compute the associated stiffness and mass matrices S and M for several typical cases.

• **Mapped Legendre approximation (2.51):** We consider the mapping (2.15) with $s = 1$. This is a special case of the general setting analyzed in Section 2.5. As suggested in [46], it is advantageous to construct basis functions using compact combinations of orthogonal functions. In this case, we set

$$\phi_k(x) = j_{s,k}^{0,0}(x) + j_{s,k+1}^{0,0}(x)$$

with $s = 1$, which satisfies $\phi_k(0) = 0$. Then, we have $\omega(x) = 2(x+1)^{-2}$, and

$$\begin{aligned}
 m_{ik} &= \int_0^\infty \phi_k(x) \phi_i(x) \omega dx = \int_{-1}^1 (L_k(y) + L_{k+1}(y))(L_i(y) + L_{i+1}(y)) dy, \\
 s_{ik} &= \int_0^\infty \phi'_k(x) (\phi_i(x) \omega)' dx = - \int_0^\infty \phi''_k(x) \phi_i(x) \omega dx \\
 &= - \frac{1}{4s} \int_{-1}^1 (1-y)^2 \partial_y \left((1-y)^2 \partial_y (L_k(y) + L_{k+1}(y)) \right) (L_i(y) + L_{i+1}(y)) dy,
 \end{aligned}$$

where $\{L_k\}$ are Legendre polynomials of degree k . By using the properties of Legendre polynomials, it is then easy to see that M is a symmetric tridiagonal matrix and S is a non-symmetric seven diagonal matrix. Hence, the system (5.2) can be efficiently solved.

We note however that a disadvantage of the mapped Legendre method is that it leads to a non-symmetric system even though the original problem (2.51) is symmetric.

• **Laguerre approximation (2.51):** We consider the approximation of (2.51) by using Laguerre functions (with the index $\alpha = 0$). The error analysis for this method is performed in Section 3.3. We set

$$\phi_k(x) = \widehat{\mathcal{L}}_k^{(0)}(x) + \widehat{\mathcal{L}}_{k+1}^{(0)}(x)$$

which satisfies $\phi_k(0) = 0$. By using the properties of Laguerre functions, it is easy to check that both the stiffness and mass matrices are symmetric and tridiagonal (cf. [47]).

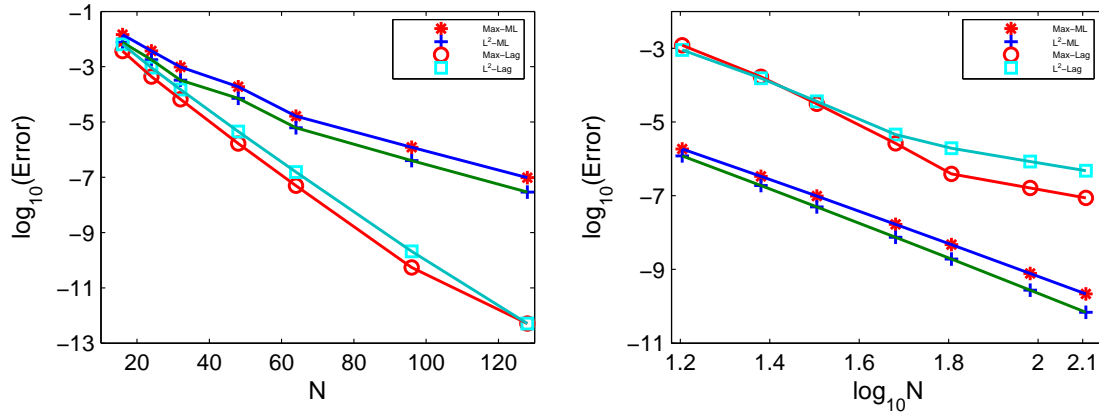


Figure 8: Convergence rates with exact solution: $u(x) = \sin(2x)\exp(-x)$ (left) and $u(x) = 1/(1+x)^{5/2}$ (right).

• **Hermite approximation for (4.27):** We consider the approximation of (4.27) by using the Hermite functions. The error analysis for this method is performed in Section 4.3. Since no boundary condition is involved, we can simply set

$$\phi_k(x) = \tilde{H}_k(x).$$

Then by using the properties of Hermite functions (4.10) and (4.13), we see that the mass matrix M is diagonal and the stiffness matrix is symmetric tridiagonal.

5.2 Numerical results and discussions

The convergence behaviors of the mapped Jacobi, Laguerre and Hermite spectral methods have been discussed in detail using the three sets of functions (2.31)-(2.33) as examples.

In order to provide a quantitative assessment, we now present some direct comparisons of mapped Legendre method (using mapping (2.15) or (2.12) with $s = 1$) against Laguerre or Hermite method.

In the following computations, we fix $\gamma = 2$ in Eq. (2.51) or (4.27). The parameters in the three sets of exact solutions are set as follows: $k = 2$ in (2.31), $h = 2.5$ in (2.32) and $k = 2, h = 3.5$ in (2.33). The numerical results are plotted in Figs. 8-10 in which “Max-ML”, “Max-Lag” and “Max-Hmt” denote respectively error in maximum norm for mapped Legendre, Laguerre and Hermite methods (similar for the L^2 notations).

Several remarks are in order: (i) For exact solutions in (2.31), Laguerre and Hermite methods converge faster; (ii) for exact solutions in (2.32), the mapped Legendre method performs much better; (iii) for exact solutions in (2.33), the Laguerre method is slightly better than the mapped Legendre method, while the Hermite method is still worse than the mapped Legendre method. We note however that the performance of Laguerre and Hermite methods can be significantly improved using a proper scaling (cf. [47, 53] and the discussion below).

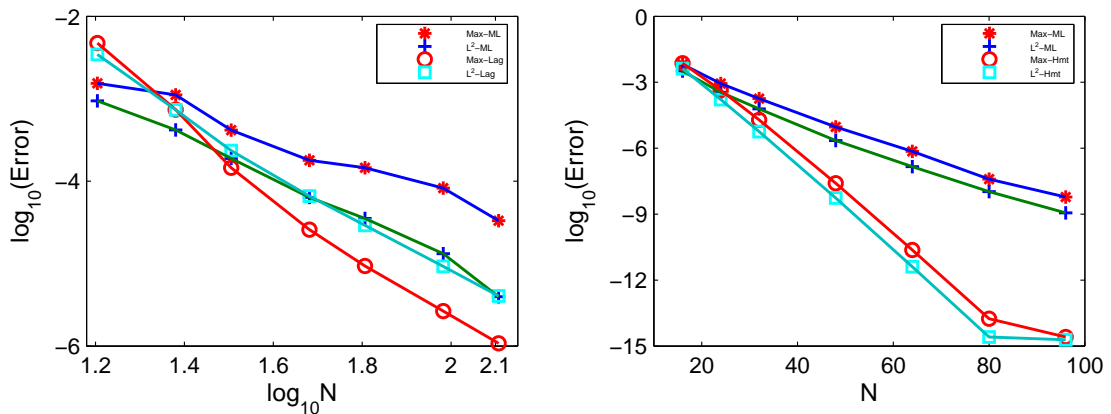


Figure 9: Convergence rates with exact solution: $u(x) = \sin 2x / (1+x)^{7/2}$ (left) and $u(x) = \sin 2x \exp(-x^2)$ (right).

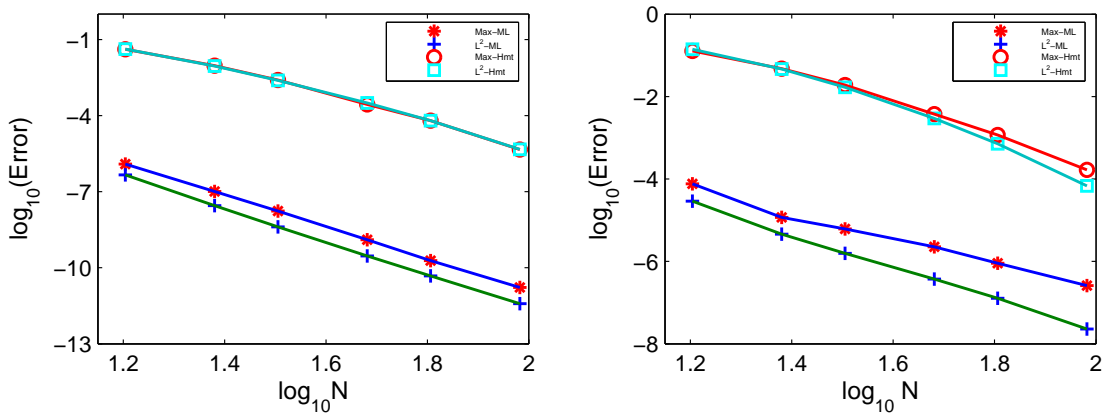


Figure 10: Convergence rates with exact solution: $u(x) = 1 / (1+x^2)^{5/2}$ (left) and $u(x) = \sin 2x / (1+x^2)^{7/2}$ (right).

6 Miscellaneous issues and extensions

We discuss in this section some miscellaneous issues and extensions related to the spectral methods in unbounded domains.

6.1 Modified Legendre-rational approximations

We notice that the mapped Jacobi polynomials, including the mapped Legendre polynomials, are mutually orthogonal in a weighted Sobolev space. Thus, their applications involve weighted formulations which are, on the one hand, difficult to analyze and implement, and on the other hand, not suitable for certain problems which are only well-posed in non-weighted Sobolev spaces. Therefore, it is sometimes useful to construct

(non-weighted) orthogonal systems from mapped Jacobi polynomials. Let us consider one such example now. We define the modified Legendre rational functions of degree l by

$$R_l(x) = \frac{\sqrt{2}}{x+1} L_l\left(\frac{x-1}{x+1}\right), \quad l=0,1,2,\dots$$

By (2.1), $R_l(x)$ are the eigenfunctions of the singular Sturm-Liouville problem

$$(x+1)\partial_x(x(\partial_x((x+1)v(x)))) + \lambda v(x) = 0, \quad x \in \Lambda, \quad (6.1)$$

with the corresponding eigenvalues $\lambda_l = l(l+1)$, $l=0,1,2,\dots$. Due to (2.2) and (2.3), they satisfy the recurrence relations

$$R_{l+1}(x) = \frac{2l+1}{l+1} \frac{x-1}{x+1} R_l(x) - \frac{l}{l+1} R_{l-1}(x), \quad l \geq 1, \quad (6.2)$$

$$2(2l+1)R_l(x) = (x+1)^2(\partial_x R_{l+1}(x) - \partial_x R_{l-1}(x)) + (x+1)(R_{l+1}(x) - R_{l-1}(x)). \quad (6.3)$$

Furthermore,

$$\lim_{x \rightarrow \infty} (x+1)R_l(x) = \sqrt{2}, \quad \lim_{x \rightarrow \infty} x \partial_x((x+1)R_l(x)) = 0. \quad (6.4)$$

By the orthogonality of the Legendre polynomials,

$$\int_{\Lambda} R_l(x) R_m(x) dx = \left(l + \frac{1}{2}\right)^{-1} \delta_{l,m}. \quad (6.5)$$

We refer to [32] and to [45] for the analysis and applications of the modified Legendre-rational spectral approximations on the half line and on the whole line, respectively. We also note that based on the same motivation and using a similar approach, a modified Chebyshev rational method, for which fast transforms are possible thanks to FFT, is developed in [28].

6.2 Irrational mappings

For many applications, e.g., in fluid dynamics and in financial mathematics, the solutions may tend to a constant or even grow with a specified rate at infinity. For such problems, variational formulations in Sobolev spaces with uniform weight or a given non-matching weight are usually not well posed. Therefore, it becomes necessary to construct orthogonal systems which match the asymptotic behaviors of the underlying problem. First effort of such kind is carried out in [11] where a rational Chebyshev method with polynomial growth basis functions is developed. A more general approach is presented in [33] where they considered the following orthogonal system:

$$I_l^{(\gamma,\delta)}(r) := \frac{1}{r^\gamma} J_l^{(\alpha,0)}\left(1 - \frac{2}{r^\delta}\right). \quad (6.6)$$

In the above, $J_l^{(\alpha,0)}(r)$ is the Jacobi polynomial of degree l with index $(\alpha,0)$. The parameter γ is chosen to match, as closely as possible, the asymptotic behavior of the function to be approximated; the parameter $\delta > 0$ is a mapping parameter which will affect the accuracy of the approximation in a way which will be made clear in Section 5; α is determined in such a way that $\{I_k^{(\gamma,\delta)}(r)\}$ form an orthogonal system in $L^2_{\omega_\sigma}(\Lambda)$, where σ is another parameter, $\Lambda = (1,\infty)$ and $\omega_\sigma = r^\sigma$. This latter condition requires that

$$\alpha = \frac{1}{\delta}(2\gamma - \delta - \sigma - 1).$$

Hence, α is *not* a free parameter. Therefore, the proposed family of orthogonal systems $\{I_k^{(\gamma,\delta)}(r)\}$ is very general and includes in particular many special cases already studied in the literature. The great flexibility afforded by the free parameters γ, δ (and σ) allows us to design suitable approximations for a large class of partial differential equations.

6.3 Scaling

For a problem whose solution decays at infinity, there is an effective interval outside of which the solution is negligible, and collocation points which fall outside of this interval are essentially wasted. On the other hand, if the solution is still far from negligible at the collocation point(s) with largest magnitude, one can not expect a very good approximation. Hence, the performance of spectral methods in unbounded domains can be significantly enhanced by choosing a proper scaling parameter such that the extreme collocation points are at or close to the endpoints of the effective interval.

For mapped Jacobi methods, this parameter is the mapping parameter s , see Section 2.1 and in particular Fig. 1. For Laguerre and Hermite spectral methods, one usually needs to determine a suitable scaling parameter β and then make a coordinate transform $y = \beta x$ (cf. [47, 53]).

To illustrate the idea, let us consider (2.51) and an accuracy threshold ε . We estimate a M such that $|u(x)| \leq \varepsilon$ for $x > M$. Then, we set the scaling factor $\beta_N = x_N^{(N)} / M$ where $x_N^{(N)}$ is the largest Laguerre Gauss-Lobatto point. Now instead of solving Eq. (2.51), we solve the following scaled equation with the new variable $y = \beta_N x$:

$$-\beta_N^2 v_{yy} + \gamma v = g(y); \quad v(0) = 0, \quad \lim_{y \rightarrow +\infty} v(y) = 0, \tag{6.7}$$

where $v(y) = u(\beta_N x)$ and $g(y) = f(\beta_N x)$. Thus, the effective collocation points $x_j = y_j / \beta_N$ (with $\{y_j\}_{j=0}^N$ being the Laguerre Gauss-Lobatto points) are all located in $[0, M]$.

An illustrative example, we consider (2.51) with the exact solution $u(x) = \sin(10x) / (1+x)^5$. In Fig. 11, we plot the exact solution and the approximations without scaling using 128 points and with a scaling factor = 15 using 32 points.

Notice from Fig. 11 that if no scaling is used, the approximation with $N = 128$ still exhibits an observable error, while the approximation with a scaling factor of 15 using

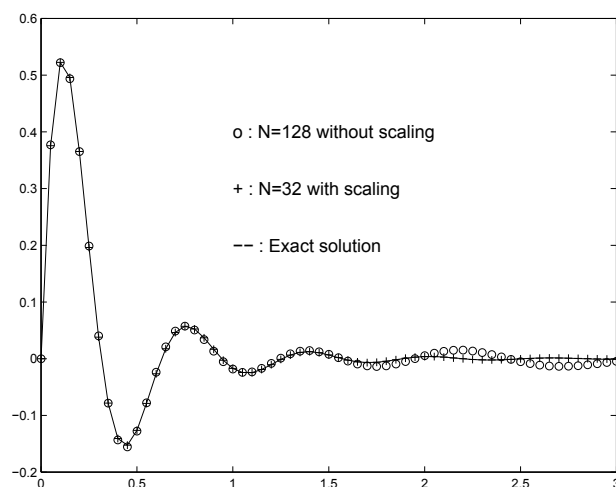


Figure 11: Exact solution against numerical solutions by (3.48) with $N=128$ (without scaling), and by solving (6.7) with $N=32$ and the scaling factor $\beta_N=15$.

only 32 modes is virtually indistinguishable with the exact solution. This simple example demonstrates that a proper scaling will greatly enhance the resolution capabilities of the Laguerre functions. In [41], a Hermite spectral method with time-dependent scaling is proposed for parabolic problems.

6.4 Other one-dimensional applications

While we have only presented analysis and implementation details for second-order model equations, the basic approximation results presented here can be used for many other applications. We refer to Boyd [11] for a review on the work before year 2000 which includes in particular many applications in oceanography. We now list some of the more recent work. In [18], a combined Hermite-finite difference method is proposed for a Fokker-Planck equation with one spatial and one phase dimension; in [36], the authors applied the Hermite spectral method for solving the Dirac equation on the whole line; in [32], a modified Legendre rational method is presented for the KdV equation in a semi-infinite interval; the same problem is also studied in [50] where a single domain Laguerre and two-domain Legendre-Laguerre method are introduced and analyzed.

6.5 Multidimensional problems

Although only one-dimensional problems are discussed in the previous sections, these one-dimensional orthogonal systems can be easily used for multidimensional problems through the usual tensor product approach. Although it is possible to use mapped Legendre methods for multidimensional problems, the analysis and implementation become complicated due the non-uniform weights involved in the variational formulation. As a

consequence, most of the work for multidimensional problems use either Laguerre or Hermite functions combined with Legendre polynomials or Fourier series.

6.5.1 Channel geometries

For problems which are set in an infinite (resp. semi-infinite) channel, it is natural to consider using Hermite (resp. Laguerre) functions in the infinite direction and Jacobi polynomials in the finite direction. For example, in [58], the authors studied a Laguerre-Legendre approximation to the 2-D Navier-Stokes equations in the streamline diffusion-vorticity formulation in a semi-infinite channel, while in [2] the authors studied approximation of the 2-D Stokes equations in primitive variables by a Laguerre-Legendre method. More precisely, a complete numerical analysis with an explicit estimate on inf-sup condition, and a detailed numerical algorithm as well as numerical results are presented in [2].

6.5.2 Exterior domains

For problems which are set in exterior domains, it is convenient, for a 2-D domain exterior to a circle, to use polar coordinates and a Laguerre-Fourier approximation (cf. [37]); and for a 3-D domain exterior to a sphere, to use spherical coordinates and a Laguerre-spherical harmonic approximation (cf. [57]). In these cases, the analysis is a bit more complicated due to the coordinate transforms but can still be carried out using essentially the approximation results presented in this paper.

6.5.3 Special applications of Laguerre and Hermite functions

Since Laguerre and Hermite functions are respectively eigenfunctions of Laguerre and Hermite Sturm-Liouville problems which play important roles in physics and mechanics, they can be especially useful for problems which involve the Sturm-Liouville operators associated with the Laguerre or Hermite functions. For example, the Laguerre and Hermite functions are particularly effective for solving Schrödinger type equations, in particular Gross-Pitaevskii equation for Bose-Einstein condensates, since the properly scaled Laguerre (or generalized-Laguerre) and Hermite functions are eigenfunctions of its linear operator with special potential functions (cf. [4, 5], see also [55]).

7 Concluding remarks

In this paper we presented a unified framework for analyzing the spectral methods in unbounded domains using mapped Jacobi, Laguerre and Hermite functions. Using these error estimates, we made a detailed comparison of the convergence rates of these spectral methods for solutions with typical decay behaviors. The following general observations can be made related to the convergence rates:

- For smooth functions which decay exponentially fast at infinity, all methods converge exponentially.

- For functions with singularities inside the domain, e.g., $u^{(j)} \in L_{loc}^2(\Lambda)$ for $j=0,1,\dots,k$ but $u^{(k+1)} \notin L_{loc}^2(\Lambda)$, the mapped Jacobi methods lead to an optimal convergence rate of k (assuming u decays sufficiently fast at infinity) while Laguerre and Hermite methods only converge with a rate of $\frac{k}{2}$.

- The mapped Jacobi methods are much more effective for functions without oscillation at infinity. More precisely,

- the mapped Jacobi methods converge faster (resp. slower) than the Laguerre method for functions **without** (resp. **with**) oscillation at infinity;
- the mapped Jacobi methods converge faster than the Hermite spectral methods for functions **with** or **without** oscillations at infinity.

Some observations related to implementations are:

- The use of Laguerre and Hermite polynomials are not advisable due to their wild behaviors at infinity. Instead, Laguerre and Hermite functions should be used.

- The mapped Jacobi rational functions are orthogonal in weighted Sobolev spaces so they lead to non-symmetric systems even for self-adjoint problems. The mapped Jacobi methods can be easily implemented in a collocation form although it leads to full matrices.

- The Laguerre (with $\alpha = 0$) and Hermite functions are orthogonal in the usual (non-weighted) Sobolev spaces and lead to symmetric systems for self-adjoint problems and with easily computable sparse systems for problems with constant or polynomial coefficients.

- A suitable choice of the mapping parameters for the mapped Jacobi method and the scaling parameters for the Laguerre or Hermite methods can greatly enhance the numerical results. The choice of the scaling parameters is particularly important for Laguerre and Hermite methods.

In summary, orthogonal systems consisting of mapped Jacobi, Laguerre and Hermite functions are all suitable tools for solving problems in unbounded domains and their approximation properties are now well understood. Mapped Jacobi methods are usually more effective, in particular for problems without oscillations at infinity, but Laguerre and Hermite methods can be made competitive with a proper choice of scaling parameters, and can be particularly effective for many special problems where Laguerre and Hermite functions are the eigenfunctions of the principle linear operator. Applications of these methods to challenging physical problems are still scarce and mostly welcome.

Acknowledgments

The work of J.S. is partially supported by the NFS grant DMS-0610646. The work of L.W. is partially supported by a Start-Up grant from NTU and by Singapore MOE Grant T207B2202 and Singapore grant NRF 2007IDM-IDM002-010.

References

- [1] J. Aguirre and J. Rivas. Hermite pseudospectral approximations. An error estimate. *J. Math. Anal. Appl.*, 304(1):189–197, 2005.
- [2] M. Azaiez, J. Shen, C.-J. Xu, and Q. Zhuang. A Laguerre-Legendre spectral method for the Stokes problem in a semi-infinite channel. *SIAM J. Numer. Anal.*, accepted.
- [3] I. Babuška and B.-Q. Guo. Optimal estimates for lower and upper bounds of approximation errors in the p -version of the finite element method in two dimensions. *Numer. Math.*, 85(2):219–255, 2000.
- [4] W. Bao and J. Shen. A generalized-Laguerre-Hermite pseudospectral method for computing symmetric and central vortex states in Bose-Einstein condensates. *J. Comput. Phys.* submitted.
- [5] W. Bao and J. Shen. A fourth-order time-splitting Laguerre-Hermite pseudo-spectral method for Bose-Einstein condensates. *SIAM J. Scient. Comput.*, 26:2110–2028, 2005.
- [6] C. Bernardi and Y. Maday. Spectral method. In P. G. Ciarlet and L. L. Lions, editors, *Handbook of Numerical Analysis, V. 5 (Part 2)*. North-Holland, 1997.
- [7] J. P. Boyd. The rate of convergence of Hermite function series. *Math. Comp.*, 35(152):1309–1316, 1980.
- [8] J. P. Boyd. The optimization of convergence for Chebyshev polynomial methods in an unbounded domain. *J. Comput. Phys.*, 45(1):43–79, 1982.
- [9] J. P. Boyd. Orthogonal rational functions on a semi-infinite interval. *J. Comput. Phys.*, 70:63–88, 1987.
- [10] J. P. Boyd. Spectral methods using rational basis functions on an infinite interval. *J. Comput. Phys.*, 69:112–142, 1987.
- [11] J. P. Boyd. *Chebyshev and Fourier Spectral Methods*. Dover Publications Inc., Mineola, NY, 2nd edition, 2001.
- [12] J. P. Boyd, C. Rangan, and P.H. Bucksbaum. Pseudospectral methods on a semi-infinite interval with application to the hydrogen atom: a comparison of the mapped fourier-sine method with Laguerre series and rational Chebyshev expansion. *J. Comp. Phys.*, 188:56–74, 2003.
- [13] C. Canuto, M. Y. Hussaini, A. Quarteroni, and T. A. Zang. *Spectral Methods, Fundamentals in Single Domains*. Springer-Verlag, Berlin, 2006.
- [14] C. I. Christov. A complete orthonormal system of functions in $L^2(-\infty, \infty)$ space. *SIAM J. Appl. Math.*, 42(6):1337–1344, 1982.
- [15] A. Clout and J. A. C. Weideman. An adaptive algorithm for spectral computations on unbounded domains. *J. Comput. Phys.*, 102(2):398–406, 1992.
- [16] P. J. Davis and P. Rabinowitz. *Methods of Numerical Integration*. Computer Science and Applied Mathematics. Academic Press Inc., Orlando, FL, second edition, 1984.
- [17] B. Engquist and A. Majda. Absorbing boundary conditions for numerical simulation of waves. *Proc. Nat. Acad. Sci. U.S.A.*, 74(5):1765–1766, 1977.
- [18] J. C. M. Fok, B.-Y. Guo, and T. Tang. Combined Hermite spectral-finite difference method for the Fokker-Planck equation. *Math. Comp.*, 71(240):1497–1528, 2002.
- [19] D. Funaro. *Polynomial Approxiamtions of Differential Equations*. Springer-Verlag, 1992.
- [20] D. Funaro and O. Kavian. Approximations of some diffusion evolution equations in unbounded domains by Hermite functions. *Math. Comp.*, 57:597–619, 1990.
- [21] D. Givoli. *Numerical Methods for Problems in Infinite Domains*. Elsevier, Amsterdam, 1992.
- [22] D. Givoli and J. B. Keller. A finite element method for large domains. *Comput. Methods Appl.*

- Mech. Engrg.*, 76(1):41–66, 1989.
- [23] D. Gottlieb and S. A. Orszag. *Numerical Analysis of Spectral Methods: Theory and Applications*. SIAM-CBMS, Philadelphia, 1977.
- [24] C. E. Grosch and S. A. Orszag. Numerical solution of problems in unbounded regions: coordinates transforms. *J. Comput. Phys.*, 25:273–296, 1977.
- [25] M. J. Grote and J. B. Keller. On nonreflecting boundary conditions. *J. Comput. Phys.*, 122(2):231–243, 1995.
- [26] B.-Y. Guo. *Spectral Methods and Their Applications*. World Scientific, River Edge, NJ, 1998.
- [27] B.-Y. Guo, L.-L. Wang, and Z.-Q. Wang. Generalized Laguerre interpolation and pseudospectral method for unbounded domains. *SIAM J. Numer. Anal.*, 43(6):2567–2589 (electronic), 2006.
- [28] B.-Y. Guo and Z.-Q. Wang. Modified Chebyshev rational spectral method for the whole line. *Discrete Contin. Dyn. Syst.*, pages 365–374, 2003. Dynamical systems and differential equations (Wilmington, NC, 2002).
- [29] B.-Y. Guo and C.-L. Xu. Hermite pseudospectral method for nonlinear partial differential equations. *M2AN Math. Model. Numer. Anal.*, 34(4):859–872, 2000.
- [30] B.-Y. Guo. Error estimation of Hermite spectral method for nonlinear partial differential equations. *Math. Comp.*, 68(227):1067–1078, 1999.
- [31] B.-Y. Guo and J. Shen. Laguerre-Galerkin method for nonlinear partial differential equations on a semi-infinite interval. *Numer. Math.*, 86:635–654, 2000.
- [32] B.-Y. Guo and J. Shen. On spectral approximations using modified Legendre rational functions: Application to Korteweg-de Vries equation on the half line. *Indiana Math. J.*, 50:181–204, 2001.
- [33] B.-Y. Guo and J. Shen. Irrational approximations and their applications to partial differential equations in exterior domains. *Adv. Comput. Math.*, pages DOI 10.1007/s10444-006-9020-5, 2007.
- [34] B.-Y. Guo, J. Shen, and Z.-Q. Wang. Chebyshev rational spectral and pseudospectral methods on a semi-infinite interval. *Internat. J. Numer. Methods Engrg.*, 53(1):65–84, 2002.
- [35] B.-Y. Guo, J. Shen, and Z.-Q. Wang. A rational approximation and its applications to differential equations on the half line. *J. Sci. Comp.*, 15:117–147, 2000.
- [36] B.-Y. Guo, J. Shen, and C.-L. Xu. Spectral and pseudospectral approximations using Hermite functions: Application to the Dirac equation. *Adv. Comput. Math.*, 19:35–55, 2003.
- [37] B.-Y. Guo, J. Shen, and C.-L. Xu. Generalized Laguerre approximation and its applications to exterior problems. *J. Comput. Math.*, 23(2):113–130, 2005.
- [38] B.-Y. Guo and L.-L. Wang. Jacobi approximations in non-uniformly Jacobi-weighted Sobolev spaces. *J. Approx. Theory*, 128(1):1–41, 2004.
- [39] B.-Y. Guo and Z.-Q. Wang. Legendre rational approximation on the whole line. *Sci. China Ser. A*, 47(suppl.):155–164, 2004.
- [40] Y. Liu, L. Liu, and T. Tang. The numerical computation of connecting orbits in dynamical systems: a rational spectral approach. *J. Comput. Phys.*, 111(2):373–380, 1994.
- [41] H.-P. Ma, W. Sun, and T. Tang. Hermite spectral methods with a time-dependent scaling for parabolic equations in unbounded domains. *SIAM J. Numer. Anal.*, 43(1):58–75, 2005.
- [42] Y. Maday, B. Pernaud-Thomas, and H. Vandeven. Reappraisal of Laguerre type spectral methods. *La Recherche Aérospatiale*, 6:13–35, 1985.
- [43] G. Mastroianni and D. Occorsio. Lagrange interpolation at Laguerre zeros in some weighted uniform spaces. *Acta Math. Hungar.*, 91(1-2):27–52, 2001.
- [44] D. Nicholls and J. Shen. A stable, high-order method for two-dimensional bounded-

- obstacle scattering. *SIAM J. Sci. Comput.*, to appear.
- [45] Z.-Q. Wang and B.-Y. Guo. Modified Legendre rational spectral method for the whole line. *J. Comput. Math.*, 22(3):457–474, 2004.
 - [46] J. Shen. Efficient spectral-Galerkin method I. direct solvers for second- and fourth-order equations by using Legendre polynomials. *SIAM J. Sci. Comput.*, 15:1489–1505, 1994.
 - [47] J. Shen. A new fast Chebyshev-Fourier algorithm for the Poisson-type equations in polar geometries. *Appl. Numer. Math.*, 33:183–190, 2000.
 - [48] J. Shen. Stable and efficient spectral methods in unbounded domains using Laguerre functions. *SIAM J. Numer. Anal.*, 38:1113–1133, 2000.
 - [49] J. Shen and L.-L. Wang. Error analysis for mapped Legendre spectral and pseudospectral methods. *SIAM J. Numer. Anal.*, 42:326–349, 2004.
 - [50] J. Shen and L.-L. Wang. Laguerre and composite Legendre-Laguerre dual-Petrov-Galerkin methods for third-order equations. *Discrete Contin. Dyn. Syst. Ser. B*, 6(6):1381–1402, 2006.
 - [51] J. Shen and L.-L. Wang. Analysis of a spectral-Galerkin approximation to the Helmholtz equation in exterior domains. *SIAM J. Numer. Anal.*, 45:1954–1978, 2007.
 - [52] G. Szegő. *Orthogonal Polynomials*, 4th edition, volume 23. AMS Coll. Publ., 1975.
 - [53] T. Tang. The Hermite spectral method for Gaussian-type functions. *SIAM J. Sci. Comput.*, 14:594–606, 1993.
 - [54] Z.-Q. Wang and B.-Y. Guo. A rational approximation and its applications to nonlinear partial differential equations on the whole line. *J. Math. Anal. Appl.*, 274(1):374–403, 2002.
 - [55] J. A. C. Weideman. Spectral differentiation matrices for the numerical solution of Schrödinger's equation. *J. Phys. A*, 39(32):10229–10237, 2006.
 - [56] J. A. C. Weideman and S. C. Reddy. A MATLAB differentiation matrix suite. *ACM Trans. Math. Software*, 26(4):465–519, 2000.
 - [57] X.-Y. Zhang and B.-Y. Guo. Spherical harmonic-generalized Laguerre spectral method for exterior problems. *J. Sci. Comput.*, 27(1-3):523–537, 2006.
 - [58] C.-L. Xu and B.-Y. Guo. Mixed Laguerre-Legendre spectral method for incompressible flow in an infinite strip. *Adv. Comput. Math.*, 16(1):77–96, 2002.